A Digital Computer Code for Calculating Reentry Phenomena in the Heated FBR Core Coolant Channel

February, 1972

HITACHI, LTD.

〒319-1184　茨城県那珂郡東海村大字村松4番地49
核燃料サイクル開発機構
技術展開部　技術協力課

Inquiries about copyright and reproduction should be addressed to:
Technical Cooperation Section,
Technology Management Division,
Japan Nuclear Cycle Development Institute
4-49 Muramatsu, Tokai-mura, Naka-gun, Ibaraki, 319-1184
Japan

A Digital Computer Code for Calculating Reentry Phenomena in the Heated FBR Core Coolant Channel *

Abstract

A new code system of safety analysis for the FBR core accidents is being developed by Power Reactor and Nuclear Fuel Development Corporation. Supporting this project, Hitachi Research Laboratory of Hitachi Ltd. developed a digital code, SUSIE, in 1970, to explain the sodium boiling phenomena in a single channel by "single bubble model".

Here, the above code is improved to calculate the reentry phenomena of sodium into the boiled channel in case of heat up accidents of FBR core. The new code SUSLE - II can calculate the time intervals from disturbance initiation to sodium boiling, growth rate of the bubble, condition of sodium reentry temperature distribution of the fuel and so on.

Feb., 1972

Naoki Sakurama **
Seiichiro Sakaguchi **
Shunsuke Uchida **

---

* Work performed under contracts between Power Reactor and Nuclear Fuel Development Corporation and Hitachi, Ltd.

** Hitachi, Ltd.

C O N T E N T S

PREFACE

With respect to the sodium cooled fast breeder reactor (FBR) which is now being developed, if no immediate and appropriate measures or action are taken in case of any loss of in-core coolant flow or an unexpected increase of in-core power output by some reason, the accident may rapidly precipitate and may cause the core melting, and further, even a serious super-criticality accident.

Especially, even in case of a local channel blockage accident whose occurrence within a core can not be absolutely deniable, there is at present no absolute guaranty of ite immediate prevention from propagating into a further serious accident.

With the conventional safety calculation, as it was difficult to evaluate sufficiently the progress and behavior of this type of accidents, it has been a general practice, after having evaluated and analized the possible causes of accident, to analize the explosion energy assuming that a substantial part of the core had melted and re-assembled. However, the quantitative evaluation of the relation between the causes of accident and the super-criticality accident has not yet been sufficiently conducted.

In order to make clear of this relationship, and at the same time, to assure by means of calculation that these super-criticality accidents would never occure again, and by doing so, to eliminate them from the future safety examination after the present FBR prototype "MONJU", the Power Reactor and Nuclear Fuel Development Corporation (hereinafter called PNC) has organized a special technical committee to have it engage in the development of a comprehensive general code for analysis of in-core accidents of the sodium cooled FBR.

At the first stage of the development of this integral code, for the preparation of a prototype of this general code, the following several codes are being prepared as a sub-routine of the general code: An analysis code for various troubles leading to major accidents, a code to calculate the development of accidents, and a code to calculated the energy release.

Hitachi Ltd. had undertaken under contract with PNC in 1970 the development of an in-core fuel channel sodium boiling analysis code as

a sub-routine of this general code, and prepared a code "SUSIE" to calculate a single channel sodium boiling by a single bubble model.

SUSIE uses the single bubble model (piston model), which is supposed to best fit the experiment data among the number of available boil analysis models at present, to analize the sodium boiling phenomena occurring in the fuel channel as the result of an in-core power generation (calorific value) variation caused by the reactivity input.

In 1970, a SUSIE prototype was prepared, and it has become possible to calculate the in-channel temperature variation from the time of an accident occurrence in the channel to the time of void appearance, the growth of void after the commencement of boil, and the temperature change in the fuel and on the cladding materials. But SUSIE did not cover any re-entry of sodium once it had escaped from the channel. For this reason, in 1971, an improvement of SUSIE was undertaken with more emphasis on its performance to calculate the reentry into the sodium channel after its boiling. With respect to sodium reentry into channel, as there were considered existing several problems relating to determination of types of model, establishment of reentry conditions, etc., these problems were first taken up for further study. This report, therefore, will cover the handling of reentry, the basic formula and the description of the code, its characteristic features, the form of input and output and how to use them, and the calculation result and its evaluation. By calculating reentry, it can be expected from SUSIE that after the escape of void, the temperature rise on the cladding materials which used to be calculated by heat insulation can be substantially moderated.

1. Characteristic Features of SUSIE-II

SUSIE-II is an improved version of the sodium boil analysis code SUSIE developed by Hitachi Ltd. in 1970. As to the basic formulas of calculation, these will be described in the later chapter. Anyway, the improved version SUSIE-II is quite similar in substance to the older version SUSIE, except in the points that while SUSIE was unable to sufficiently calculate the vibration at the end-faces of void and the cooling efficiency by sodium reentry after void escaped from the channel, SUSIE-II is able to calculate all these phenomena. As said before, SUSIE-II is after all an improved version of SUSIE added with several new calculation techniques and performance functions.

Table 1-1 represents the major differences in comparison with SUSIE-II and SUSIE.

1-1. Calculation Models

i). As indicated by Fig. 1-1, a cylindrical from model is considered, where the liquid film (emulsion) and sodium flow surround the fuel pins and the cladding. The channel's outer diameter is determined by the cross section of the sodium flow channel.

ii). The fuel, clad and the liquid film are considered as fixed. Only the sodium other than liquid film flows.

iii). On the fixed side, the thermal transfer in the axial direction is ignored.

iv). The temperature distribution of sodium in the channel is measured and calculated by this model until an actual boiling takes place.

1-1.2. On the sodium side (Calculation after boiling takes place).

i). As shown by Fig. 1-2, the liquid film is adhered to the cladding, and changes its thickness as void grows.

ii). The film thickness changes depending on the axial direction mesh, while both keep changing every now and then.

iii). When the film thickness comes to zero, heat insulation on the surface of the cladding materials is considered.

1-1.3. Connection Between Heat Generating Side and Sodium Side.

i). By utilizing the thermal flow flux on the surface of the liquid film, the temperature of the fuel pins, cladding and of the liquid film is obtained with the model of Fig. 1-1.

ii). Utilizing the temperature on the surface of the liquid film, the void pressure, volume, sodium temperature and the thermal flow flux on the surface of the liquid film are sought.

iii). Items of i) and ii) are calculated every hour repeatedly.

1-2. Reentry Models.

1). Calculation on the heat generating side does not change.

ii). The void which comes out from the channel's exit is considered to go up (come down) inside the assumed channel.

iii). The cross section of the assumed channel is the same as that of the actual channel, and the temperature of its wall is constant (equivalent temperature to that of the bulk sodium at the channel's exit) in the axial direction.

iv). The sodium vapor condenses at the upper part of the assumed channel. Here, it assumed channel. Here, it assumed the void pressure declines and this pressure decline causes sodium reentry into channel takes place.

v). Calculate the position of the end-faces of void and the void pressure inside both the channel and the assumed channel.

1-3. Time Mesh.

In order to calculate the vibration phenomenon occurring with the reentry, as the conventional method of calculation by means of a certain time mesh size was difficult to obtain a satisfactory result, the calculation was performed by changing the time mesh size maintaing the void pressure $\triangle P_v$ within a certain limited range.

1.4. Accident Causing Factors.

i). Variation of heat generation: The initial distribution of heat generation distribution shouled be given, and the time variation of the absolute value is determined by the function which is given as input.

ii). Channel blockage: The flow volume variation function arising from channel blockage should be given by input.

iii). Pressure variation at channel inlet: The pressure variation function at the channel's inlet arising from some pump troubles should be given by input.

1-5. Other Improved Points from SUSIE.

i). As the surface temperature of the liquid film was unstable fluctuating largely at the time of vapor condensation, the clad and the liquid film were combined to form a mean value of one mesh. In reality, it is assumed that the temperature gradient can be negligible.

ii). Consideration of vapor condensation on the boundary surfaces below and above void.

As the temperature on the boundary surfaces below and above void was high, a vapor feeding from this area was also considered. The calculation technique is entirely the same as in the case of evaporation from the liquid film. For the evaporation surface area, the channel cross section is taken.

iii). Change of liquid film thickness.

The thickness of the liquid film changes according to time and location. Assuming the thickness $S(t)$ of the liquid film at a certain hour (t) as:

$$S(t + \triangle t) = S(t) - \delta \triangle t \qquad (1\text{-}1)$$

Where, δ : Variation rate of the liquid film thickness by vaporization and condensation.

It is assumed that the liquid film thickness at the mesh point on the cladding side including the void's end-face when void expands and grows up is determined by the following process. In this case, the liquid film thickness inside one mesh is considered uniform:

$$S(t + \triangle t) = \left[S(t) + (So - S(t)) \times \triangle Z/(Z + \triangle Z) \right] - \delta \triangle t \qquad (1\text{-}2)$$

Where, So: Initial film thickness

Z: Length of void including its end-face at the time t in the mesh.

$\triangle Z$: $v \triangle t$.

v: Velocity of the end-face.

This hypothesis can be more precisely expressed by the following drawings:

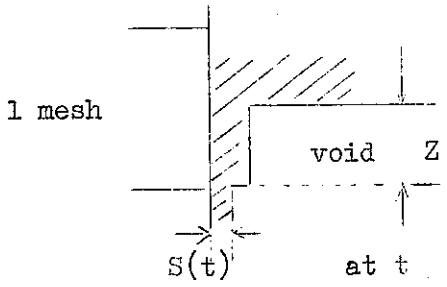

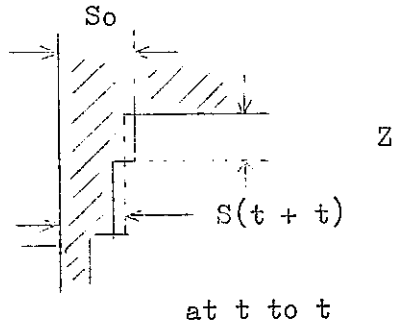

2. Reentry Models and Reentry Conditions.

2-1. Study on Reentry Models.

The reentry model used in SUSIE-II was referred to in the previous chapter. There are several models considered other than those used for this code. A model as is shown in Fig. 2-1 was studied with respect to the handling of void outside the channel outlet.

i). This is a model whereby it is considered that void is extended for the same cross section at the upper section (lower section) of the channel, and it is assumed a condensation takes place on the surface due to the temperature difference between the vapor inside void and the liquid surface, and a hypothetic channel is connected with the extended portion of the model channel.

ii). It is assumed that all such vapor of void which has escaped outside from the upper or lower part of the channel will immediately condense, but the details of condensation process will not be considered at this time here. By this, the void end-face will never goes out of the channel's outlet.

iii). It is assumed that the void is ejected out in a specific form the channel's exit. But its form has not been determined yet. Therefore, drawing attention on its surface area, the surface area is calculated by multiplying the surface area of void which is out from the model's exit by an appropriate factor, which is studied as a parameter.

The liquid film thickness which contributes to vaporization has a limit. When there is no liquid film, evaporation will cease, and soon condensation will exceed evaporation, and as the result, the void pressure will decline.

The models given by the above items i), ii) and iii) are respectively to obtain the void pressure by the vaporization and condensation balance, and are considered in the same handling in principle. Fig.2-1 shows the quantitative behavior of vaporization and condensation of each model.

For SUSIE-II, as approximately the similar models can be considered from the models given in items i), ii) and iii) it was decided to use preliminarily the model of i). But as it is not so difficult to change

i) model for iii) model, a study may be made to switch to model iii) in some future.

2-2. Reentry Conditions.

As void grows and expands from the void area into the sub-cooled area, the condensation volume will surpass the vaporization volume, and thus the pressure inside void will decline. When void pressure declines smaller than the external pressure, the growing speed of void will slow down, and soon the growth stops. Further then, sodium will make a reentry into void affected by the external pressure difference. Consequently, the required conditions for reentry are:

P_2 (exit pressure) $> P_v$ (void pressure)

In the actual case, when considering the inertia of the sodium liquid column above and below the void, reentry is considered to take place at the time somewhat delayed from the moment of P_2 P_v.

In this case, it is difficult to define the length of the liquid column when void is outside of the channel's exit. However, with SUSIE-II, the length from the void end-face to the channel's exit is taken as the length of the liquid column so long as the void end-face remains inside the channel. Although, the liquid column length will become shorter as the void end-face approaches closer to the channel's exit. But in this model, the one-mesh length of the liquid column will be taken as the minimum value. Also with respect to the liquid column length in case that void has escaped outside from the channel's exit, this method will be extended, and one-mesh length will be taken as the length of the liquid column. In this code, the equations of motion as given in the following chapter are solved by utilizing the above stated hypothesis.

3. Basic Formulas for Calculation.

This chapter describes the basic calculation formulas which are used in this code. Calculations are performed separately on the heat generating side and on the sodium side. But so long as no void is involved on the heat generating side, it is possible to calculat the sodium flow on this side, and there is no need of using the sodium side calculation until sodium boiling takes place. After the commencement of boiling, the heat-generating side calculation will cover up to the liquid film while the sodium volume including void belongs to the sodium-side calculation.

The heat generation calculation after the commencement of boiling is further divided into two. Namely, the fuel section heat up calculation and the clad calculation covering the cladding and the liquid film. The reason for this division is to keep the key to a certain level of frequency for the sake of calculation, and also to shorten the calculation time. The basic formulas are the same regardless of the division.

3-1. Calculation of Heat Generating Side.

Fuel:

$$\frac{\partial T}{\partial t} = \frac{1}{C\rho}\left\{\frac{k}{r}\frac{\partial}{\partial r}\left(r\frac{\partial}{\partial r}T\right) + Q\right\} \qquad (3\text{-}1)$$

Where, T: Temperature (^{o}C)

Q: Heat generation rate ($Kcal/m^2h$)

k: Thermal conductivity ($Kcal/m\ h\ ^{o}C$)

C: Specific heat ($Kcal/kg\ ^{o}C$)

ρ: Density (Kg/m^3)

t: Time (h)

r: Distance from the center of fuel (m)

Between fuel and clad:

$$q_G = h_G\,(T_F - T_c) \qquad (3\text{-}2)$$

Where, q_G: Thermal flux between fuel and clad.

h_G: Gap conductance.

T_F: Fuel surface temperature.

T_c: Clad internal temperature.

Cladding and liquid film:

$$\frac{\partial T}{\partial t} = \alpha\left\{\frac{1}{r}\frac{\partial}{\partial r}\left(r\frac{\partial}{\partial r}T\right)\right\} \qquad (3\text{-}3)$$

Between liquid film and sodium:

$$q_L = h_L (T_W - T_N) \tag{3-4}$$

Where, q_L: Thermal flux from the liquid film.

h_L: Heat transfer coefficient on the surface of liquid film.

T_W: Film surface temperature.

T_N: Sodium temperature.

Heat transfer coefficient:

$$h_L = K\ Nu/D \tag{3-5}$$

$$Nu = 5.333 + 0.019 * (Pe^{0.8}) \tag{3-6}$$

Where, Nu: Nusselt number

D: Equivalent diameter

Pe: Pecle number.

Sodium:

$$\frac{\partial T}{\partial t} = \frac{\partial T}{\partial Z^2} + \frac{\ell}{S} \frac{2\pi r_\ell q_L}{\rho} - \frac{\partial}{\partial Z} \left\{ T \frac{W}{\rho S} \right\} \tag{3-7}$$

Where, α: Thermal diffusivity

Z: Distance from channel entrance (m)

r_ℓ: Liquid film's outer radius (m)

S: Channel's cross section (m^2)

ρ: Sodium density (kg^*/m^3)

W: Flow volume (kg^*/h)

The quantities or volumes under a regular or stationary state are obtained by use of the equations of (3-1) - (3-7), and then introduced into the calculations with the change of flow or heat generation rate. On the occasion, the temperature at the channel entrance flow and heat generation rate should be given as input.

3-2. Calculation on Sodium Side.

Void section.

Evaporation volume:

$$\mathring{n} = \frac{f_k}{1-0.5\ f_k} \frac{1}{\sqrt{2\pi R/A}} \left\{ \frac{P_{fs}}{\sqrt{T_f}} - \frac{P_{vs}}{\sqrt{T_v}} \right\} \tag{3-8}$$

Where, $\dot{n}$: Evaporation volume ($Kg^*/m^2 \cdot h$)

h_{fg}: Evaporation latent heat ($Kcal/kg^*$)

f_k: Condensation coefficient

R: Gas constant ($Kg \ m/mol \ ^oC$)

T_f: Film surface temperature (^oC)

T_v: Void temperature (^oC)

$P_{ts} = f(T_f)$: Saturation relative equation (Kg/m^2)

$P_{vs} = f(T_v)$: Saturation relative equation (Kg/m^2)

A: Sodium weight per mol (kg^*/mol)

Thermal flux:

$$q_v = h_{fg} \cdot \dot{n} \tag{3-9}$$

Increase of vapor in void:

$$\frac{dN}{dt} = \int_{surface} \dot{n} \, ds \tag{3-10}$$

Status equation:

$$P_{vs}V = MRT_v/A \tag{3-11}$$

Where, V: Volume of void (m^3)

N: Vapor weight of void (kg)

Increase in volume:

$$dV/dt = (v_1 - v_2) \times S \tag{3-12}$$

Where, S: Channel cross section (m^2)

v_1: Moving speed of void's upper end-face (m/h)

v_2: Moving speed of void's lower end-face (")

Flow volume:

$$W_1 = \rho S v_1 \tag{3-13}$$

$$W_2 = \rho S v_2 \tag{3-14}$$

Where, W_1, W_2: Sodium flow at upper and lower part of void (kg/h)

Sodium section.

Momentum equations:

$$\frac{dv_1}{dt} = \frac{P_v - P_1}{\rho \ h_1} + g - \frac{\lambda_1 \ v_1 \ |v_1|}{2 \ D} \zeta v_1 |v_1| \tag{3-15}$$

$$\frac{dv_2}{dt} = \frac{P_v - P_1}{h_1} - g - \frac{\lambda_2 v_2 |v_2|}{2D} - \zeta v_2 |v_2| \qquad (3\text{-}16)$$

Where, P_v: Void pressure (kg weight /m^2)

P_1: Pressure at channel entrance (kg weight /m^2)

P_2: Pressure at channel exit (kg weight /m^2)

$h_i = h_{oi} - \int_o^t v_i dt \quad (i = 1.2)$

h_{oi}: Length of sodium column (m)

λi: Pressure loss coefficient

ζi: Pressure loss coefficient at the blocking point in the channel.

Energy equations:

$$\frac{\partial T}{\partial t} = -\frac{q_v}{\Delta Z \rho C_p} + \frac{4Dq}{(D-2\ell)^2 \rho C_p} + \frac{\alpha}{\Delta Z} \frac{\partial T}{\partial Z} \qquad (3\text{-}17)$$

$$\frac{\partial T}{\partial t} = \frac{4Dq}{(D-2\ell)^2 \rho C_p} + \alpha \frac{\partial T}{\partial Z^2} \qquad (3\text{-}18)$$

Where, equation of (3-17) is for the gas-liquid boundary interface equation, while equation of (3-18) is for the equation in other positions.

q_v: Void's thermal flux into void (Kcal/m^2 h)

q : Thermal flux from the liquid film (Kcal/m^2 h)

ℓ : Film thickness (m)

C_p: Specific heat (Kcal/Kg ^oC)

According to the calculation on the sodium side, after the liquid film surface temperature is given by heat-generation calculation, the equations of (3-8) - (3-16) are employed for calculation of the growth of void, then the sodium temperature is sought by equations (3-17) and (3-18).

3-3. Time Mesh.

The time mesh t for calculation is given the maximum value, and if it does not satisfy the follwoing equation, it will be made smaller to satisfy the equation:

$$\varepsilon_1 \leqq \Delta P_v / P_v \leqq \varepsilon \qquad (3\text{-}19)$$

Where, ϵ_1 , ϵ_2 : Upper and lower limit of pressure fluctuation.

$\triangle P_V$: Pressure fluctuation of void.

P_V: Void pressure.

3-4. Thickness of Liquid Film.

The initial film thickness is S_0.

i). The film thickness $S(t)$ at the mesh point with no void end-face included is obtained by the following formula:

$$S(t + \triangle t) = S(t) - \delta \triangle t \tag{3-20}$$

Here, δ : The film thickness which changes at each time unit (m/h)

$$\delta = \dot{n} A/\rho \tag{3-21}$$

ii). The film thickness at the mesh point with void end-face included (at the time of void growth):

$$S(t + \triangle t) = \left[S(t) + \frac{S_0 - S(t)}{(Z + \triangle Z)} \triangle Z \right] - \delta \triangle t \tag{3-22}$$

$$\triangle Z = v \triangle t \tag{3-23}$$

Here, Z: Void length in the mesh at t (m)

v: Moving speed of void end-face (m/h)

4. Description of Calculation Code

The constituting sub-routines of SUSIE-II are the same as in the case of SUSIE. But the details of each sub-routine is remodeled for calculation use. Fig. 4-1 shows the block drawing of SUSIE-II.

The functions of each sub-routine are given as follows:

MAIN: Total control of Fig. 4-1 and adjustment of time mesh width.

INPUT: Input of data.

OUTPUT: Output prior to boiling.

STEADY: Temperature calculation in a stationary state.

HEATUP: Temperature calculation at transient time (only fuel temperature calculation after commencement of boiling).

NABØIL: Void growth after commencement of boiling, temperature calculation of sodium, and the output after boil commencement.

CLAD : Themperature calculation of the cladding and the liquid film after boil commencement.

FLOWRT: Function of flow fluctuation.

HEATVL: Function of heat generation change.

PRESSF: Function of pressure at channel entrance.

PRØPNA: Na physical property values.

PRØPFL: Fuel's physical property values.

PRØPSS: Stainless steel's physical property values.

The adjustment index NNVØID is zero under a stationary state until boiling takes place. After the commencement of boiling, it is NNVØID = 1.

When it is NNVØID = 1, namely, to be the time of boil commencement, is when the maximum temperature of sodium exceeds the boiling temperature plus a super heat temperature (given by an input).

5. Forms of Input and Output and Their Descriptions

5-1. Input Format.

The input data of SUSIE-II is divided into the "library data" and the "normal data". The library data are used to obtain the relation between saturation pressure and saturation temperature in the sub-routine PRØPNA, and are sufficient to make only one read-in prior to the read-in of the normal data. Table 5-1 shows the library data currently used by SUSIE-II.

The input format of the normal input data (hereafter called "input data") is as shown by Table 5-2, and the example of the actual input data writing is as shown by Table 5-3.

As for the accident factors, it is deviced that the user himself prepares the necessary functions of which coefficients are the input. Already a number of functions have been prepared and are usable any time. The types of function and the option codes are listed in Table 5-4.

The input limitation of SUSIE-II are as follows:

i) Radial direction mesh number $\leqq$ 20.

ii) Axial direction mesh number $\leqq$ 100.

iii) Axial direction region number $\leqq$ 10.

5-2. Output Format.

Table 5-5 shows an example of output. This is made during the sub-routine NABØIL after the commencement of boiling.

The meaning of the codes are given as follows:

SEC: Time of boil commencement (sec)

I : Time mesh number after boil commencement.

TIME: Time after occurrence of an accident. (sec)

TMESH: Time mesh width at I. (sec)

Z_1, Z_2: Location of void's lower end-face (1) and its upper end-face (2) (m)

W_1, W_2: Moving speed of each void face (m/sec)

DZ: Length of void (m)

PGAS, TGAS, MGAS: Void's gas pressure (Kg/m^2), temperature ($^\circ C$), and mol number.

LØW TEMLQD, UP TEMLQD: Sodium temperature at upper and lower liquid columns. (The position is taken from void's end-face).

TFUEL CENTER: Temperature in the center of fuel (^{o}C).

TFUEL SURFACE: Temperature on the surface of fuel (^{o}C).

TCLAD: Temperature of the clad (^{o}C).

TFILM: Temperature on the liquid film surface (^{o}C)

SFILM: Thickners of liquid film (m)

QFILM: Thermal flux from liquid film (Kcal/ m^2 h)

6. Result of Sample Calculation and Its Evaluation

6-1. Evaluation of Input Data.

The following items were evaluated as the possible factors to affect sodium reentry:

(1) Initial super heat

(2) Effective radius of the initial boiling nucleus

(3) Condensation coefficient

(4) Thickness of the initial residual liquid film.

The initial super-heat of item (1) is the difference between the liquid temperature required for occurrence of a boil and the saturation temperature, and may be defined by the following equation:

$$\triangle Ts \; ; \; T_{\ell} \; - \; T_{sat} \qquad (6\text{-}1)$$

Here, $\triangle Ts$: Initial super heat

T_{ℓ}: Liquid temperature at the beginning of boil

T_{sat}: Saturation temperature corresponding to the liquid pressure at the point where a boil takes place.

The value of an initial super heat is said to be especially high with a liquid metal like sodium. But the numerous available experimental data vary greatly. So, in order to determine and grasp quantitatively what factors are affecting, a number of researchers are devoting their efforts in this work, and it is considered the following as the possible affecting factors; impurities contained in sodium such as, for example, sodium oxide, argon gas, the surface conditions of the heat transferring area (coarseness or material difference), thermal flux, pre-boil temperature and pressure histories, etc.

In the calculation, the temperature value of 50°C was used. As to the effective radius of initial boiling nucleus of item (2), there is no other way than to derive it by an inverse deduction by the following equation which is theoretically introduced from a dynamic balance equation, and Clapeyron-Clausius equations. But at the present stage where the experimental values of super-heat so highly vary, it may be inevitable that an estimation of boiling nucleus radius is not quite accurate. Namely;

$$\triangle Ts = \frac{2R_V \, Ts^2 \sigma}{J h_{fg} \; r_c \; P_s} \qquad (6\text{-}2)$$

Where, $\triangle$ Ts: Initial super-heat required for bubble production (^{o}C)

Ts: Saturation temperature (^{o}K)

σ : Surface tensile force (Kg/m)

h_{fg}: Evaporation latent heat (Kcal/Kg*)

Ps: Saturation pressure (Kg/m^2)

r_c: Effective radius of boiling nucleus (m)

J: Joule's conversion coefficient (Kg m/Kcal)

As no r_c value estimation of sodium can be found in any of the available literatures, a study-case of potassium which is quite resembled to sodium in property was quoted, and r_c value was indicated by Hoffman [3] and others as distributing in between 10^{-2} mil and 3mil (namely from 0.25 μ to 75 μ). As to sodium, therefore, a value of 100 μ was employed for the calculation as indicating the value of the above order.

The value of condensation coefficient of item (3) is presently being determined both theoretically and experimentally through the research and study of water vaporization. But unfortunately, the experimental values are yet varying largely because of some problems of measuring technique. According to the study of Miils & Seban, [4] it is stated that the reason for variation from 1 to 0.002 was because of poor arrangement and adjustment of the experimental values, that when these were readjusted, all the values indicated close to 1, and that it was unbelievable that they should depart too far from 1.

With respect to sodium, there has been performed no similar study except such a study-case [5] which was undertaken by use of a boil analysis code NEMI by a single bubble model prepared and made in Italy to obtain by a parametric change of the condensation coefficient, a value of 0.01 for the condensation coefficient value at the time of the void position corresponding to both the experimental and the theoretical values.

In this calculation, a value 0.1 was employed as one criterion of calculation.

The thickness of the initial residual liquid film is one of the factors which will most seriously affect the reentry phenomenon. A detailed description of this seriously affecting factor will be given in the next chapter of "calculation results". In this calculation, its effect was conspicuous in an in-core channel blockage accident on which the main emphasis of the experiment was placed.

There is a theory that the thickness of liquid film is determined from the very place of flow, and that the thickness of the bottom layer of the laminar flow within the boundary layer is that of the liquid film. In this case, however, the flow speed immediately after the boil commencement is so small that it is doubtful whether the above theory can be established. But at any rate, it can be regarded as one basis or criterion, and its thickness is sought in the following manner: According to Prandtl's boundary layer theory, the thickness of the turbulent flow boundary layer within a cylindrical tube given by;

$$\delta = 0.379\, R_e^{-\frac{1}{5}} x \qquad (6\text{-}3)$$

Where, $R_e = \dfrac{w\, x}{\nu}$

w : Average speed of flow (m/sec)

ν : Kinematic viscosity coefficient (m^2/sec)

x : Distance in the axial direction from the channel entrance (m)

R_e: Reynolds' number (-)

δ : Thickness of turbulent flow boundary layer.

There is a straight linear speed distribution region of the bottom laminar flow within the turbulent boundary area, and its thickness δ_L is; $\delta_L = 80\, (R_e)^{-\frac{2}{8}}\, \delta$ (6-4)

Where the speed of the liquid column at both ends of void is $w = 1$ m/sec, and taking the point which is 0.01m distance from the point where a bubble has produced. There, by use of the value of υ at the boiling point, $\upsilon = 2.3 \times 10^{-7}$ (m^2/S), Reynolds' numbers are;

$$R_e = 1 \times 0.01/2.3 \times 10^{-7} = 4.35 \times 10^4$$

$$\delta = 0.379\, (0.435 \times 10^5)^{-\frac{1}{5}} \times 0.01 = 4.48 \times 10^{-4} \quad (m)$$

$$\delta_L = 80 \times (4.35 \times 10^4)^{-7/8} \times 3.20 \times 10^{-4} = 2.21 \times 10^{-6} \quad (m)$$

Namely, at the initial stage, the boundary layer thickness is 0.45 mm, and the laminar flow bottom thickness is in the range of 2.2 μ both of which are extremely thin.

On the other hand, according to the sodium boiling experiment, it is assumed that the liquid film thickness at the initial stage remains at approximately 0.1 mm. For this reason, the values of 0.1mm order was employed in this calculation.

6-2. Calculation Results.

The following are the results of calculation made with use of SUSIE-II with regard to the analysis of FBR "MONJU":

The design factors required for the calculation are given in Table 6-1, and the channel dimensions and the heat generation rate distribution are given in Fig. 6-1 and 6-2 respectively.

In order to examine the parameter, initial super heat $\triangle$ Ts, initial liquid film thickness, S, condensation coefficient C, initial bubble radius r_c, and to check on the effect of other factors such as blanket heat generation rate Q_b, axial direction mesh number MZ, etc., the numbers as shown in Table 6-2 were employed as the input data.

The numbers used in Table 6-2 as the standard case are those calculated with use of the design values of MONJU reactor, $\triangle$ Ts = 50°C, S = 0.1mm, C = 0.1, r_c = 0.1mm, Q_b = 0.07 KW/cm, and MZ was divided into 10 mesh at the core and 4 mesh at the upper part of the blanket.

The axial direction pitch intervals on the side of fuel pins is about 8.9cm and on the liquid sodium side is 4.4cm for the mesh width together with the post-boil void's upper and lower liquid column. The mesh width of liquid film formed by these voids adhering to the clad is the same as the axial direction width of the clad, provided that only such points where contact with both end-face of void (piston type upper and lower ends), the length will change dependent on the movement of void.

6-2. 1. Calculation Results in Standard Case.

In this chapter the time dependency of position of void end-face, void internal pressure, sodium temperature, clad temperature, and of the liquid film thickness in a standard case are given.

(1). The time dependency of the position of void end-face and of the void internal pressure.

Fig. 6-3 represents a plot drawing expressing the post boil time lapse by second on the horizontal direction, and the upper end-face and the lower end-face of void on the vertical direction by a metric unit taking the entrance of the core as the origin of the axis of co-ordinates.

Here, assuming that a foreign substance blocking the assembly entrance, and the flow dropped down step by step to 1% of the rated capacity, and

that the blocking substance at the entrance could not be removed even after a boiling had occurred, and in all this blocking phenomenon, the diaphragmatic effect continued working. Consequently, the lower end-face of void was almost stationary. This is obviously clear from the drawing of Fig. 6-3. Hereafter, unless otherwise specifically mentioned except in the case where a pumping trouble may have occurred and a study is made on a trouble involving a possibility of void moving downward, our attention will be focused only on the upper end-face of void.

"x" marks appearing on the vertical line in Fig. 6-3 indicate the dividing position of the clad in the axial direction, and thereby, these indicate the dividing position of the liquid film when void grows up. Also, the numbers from (1) to (9) along the axial line are the labels indicating the axial direction position of the liquid film. Likewise, the numbers from (1) to (9) given in parallel with the curve of moving void upper end-face correspond to those on the axle.

The bubbles produced in the vicinity of 0.935m of the core grow acceleratedly bigger, and the upper end-face of void goes past the core into the upper section of the blanket after about 0.07 seconds, and in 0.10 seconds reaches the exit plenum passing through the upper part of the blanket. During this process, the sodium liquid column on the upper part of void is pushed out and is mixed with the sodium inside the plenum.

As explained in the aforesaid calculation model, as a hypothetic condensation of void of an ideal type at the upper plenum is considered, the gas-liquid boundary interface is to be located at about the upper part of the blanket from the point marked (9) in Fig. 6-3 to 0.12 seconds (time lapse is 0.098 sec).

Its position at 0.11 seconds reaches its peak and thereafter nose-dives downward and quickly returns to the core, and the void vanishes away in the vicinity of the bubble producing location. Its ascending velocity is obtained by the gradient given in Fig. 6-3, and against its maximum speed of about 10 m/sec, its reentry speed is much faster, precipitating at a speed of 20 m/sec.

Fig. 6-4 represents the time dependency of void's internal pressure. The pressure which has been about $1kg/cm^2$ abs prior to boiling increases to 1.85 Kg/cm^2 abs within 1m/sec with the quick growth of void.

Thereafter, the pressure gradually rises, but when the void boundary-face reaches the vicinity of 0.07 sec which is the blanket region, the pressure suddenly begins to drop with an accompaniment of vibration in the range of 200 kHz down to about 1.6 kg/cm^2 abs.

When void reaches the upper end of the blanket region, its pressure rapidly decreases due to a sudden and quick condensation which takes place at the upper plenum. When it gets down to its lowest bottom of 0.15 kg/cm^2 abs, it again starts to rise with a vibration up to a $1kg/cm^2$ abs level.

According to a standard case calculation, its reentry completes in the vicinity of 0.155 sec, and the bubbles disappear. At the time, it may be expected that some shock pressure will appear caused by the liquid column collisions. But this has not been taken into account in the case of this model.

The reason for the faster speed of reentry than at the time of ejection may be better explained by the pressure change given in Fig. 6-4. That is, it is thought that since the mass of the moving Na liquid column is initially large and becomes smaller as going upward, its initial acceleration rate is small. While at the time of its reentry, its initial mass is so small that it is quickly accelerated. The reason for void having a negative pressure is that there occurs a condensation in the core, at the blanket and at the sodium plenum, and when it is considered that at about 0.1 sec time the clad temperature makes no much change, it can be understood that the temperature distribution immediately prior to the commencement of boiling will constitute a significant factor.

The calculation result of temperature distribution in the axial direction is given as follows:

(2) Sodium temperature and time dependency of clad temperature.

Fig. 6-5 represents the time dependency of the axial direction temperature distribution of Na liquid columns at the upper part of void after commencement of boiling. That is, sodium temperatures are given along the traverse line and the axial direction positions are given along the vertical line, while time is taken in parameter. The solid line in the drawing represents the sodium temperature when void grows (ejection),

and the broken line expresses the sodium temperature distribution when void becomes smaller (reentry). What has a direct effect upon the growth and disappearance of void is the sodium temperature contacting the void's boundary-face, and the sodium temperature as the upper and lower parts of void and the clad temperature (to be further described later), which is equivalent to the temperature of liquid film, constitute a major factor. The dotted line represents the traced line of the liquid temperature, namely, void. The reason for the changes of sodium temperatures in the void boundary as going along the line in the direction of (1) → (2) → (3) → (4) → (5) → (6) → (7) → (8) → (9), is because that, in the case of ejection, what changes reverse direction such as (8) → (7) → (6) → (5) → (4) → (3) → (2) → (1) is in the case of reentry.

Fig. 6-3, which indicates a standard case, is further explained in details as follows:

Immediate after a boiling, the temperature of Na liquid column has the same distribution pattern as shown by (1) in the drawing. The maximum temperature is 950°C at the point when the boil commences, and it comes down to 895°C at the core outlet, 750°C at the blanket area, and about 730°C in the vicinity of the blanket outlet.

With the lapse of time, the Na temperature is seen rising rapidly when viewed from the co-ordinates fixed in the air. But when viewed from the co-ordinates which is fixed to the upper end-face of void, namely, Na liquid column, there is observed hardly any changes in the temperature distribution, except only a minor one in the region in transit to the blanket from the core. This fact indicates that since the phenomenon is in the level of 0.1 sec, any temperature fluctuation caused by the cladding and a heat transfer may well be ignorable.

The sodium temperature in the void boundary will rise so long as the upper end-face of void remains in the neighborhood of (3) - (4). This is considered as the result of being heated by the fuel in the core. But the temperature rise is extremely small not more than 6°C. After (5), the temperature declines, but at (9) and up to the blanket exit, it descreases by only 20°C.

The void coming out from the plenum, condenses in the channel which is hypothetically provided in the plenum, and the sodium release from the channel is cooled by the surrounding sodium plenum of 640°C temperature, and makes a reentry into the blanket area in 0.12 seconds after the boil

has taken place (refer to (8), Fig. 6-3). The temperature at that instance is 875°C at its end-face. Thereafter, as going downward the blanket, it is cooled by still lower temperature clad, and as it goes down through (7) - (6) - (5) - (4) - (3) - (2) - (1), the temperature descends further down.

As shown by Fig. 6-5, at the time of the commencement of reentry, the sodium temperature at the void boundary-face is about 860°C, while the Na liquid column temperature on the upper side of the void boundary-face is about 640°C (the extreme left end of the broken line in the drawing).

Although this temperature increases as Na liquid column flows toward the core from the blanket area, the increase volume is small, something about 25°C. The reason for the decline of sodium temperature in the void boundary even it has entered into the core is that it is cooled by the lower sodium temperature existing at the upper part of the void boundary, while the in-core heating is unable to catch it up.

Fig. 6-6 is a plot drawing arranging against time the clad temperature, which is one at a representing point of the core, and the clad temperature which is a representing point of the blanket section. In the drawing, -o-o-o- mark represents the clad temperature at a distance Z of 1.02m from the channel entrance, and *** mark is the clad temperature at the point Z = 1.39m. Also, for the sake of comparison, the void temperature is plotted in the drawing.

At the initial stage of boiling, the in-core clad temperature is higher than the void temperature, and rises at a slow pace. The temperature increase in this section upto 0.025 sec, when the upper end-face of void has not reached the position where now our attention is focused, is because of the heating by the fuel. The interval between 0.025 sec after commencement of boiling is the interval where the liquid column and the liquid film co-exist in the axial direction mesh of the clad to which now our attention is focused, and the clad temperature has increased some degree due to the proportinate balance between the film section and the column section. At the a-mark in the drawing which is a 0.045 sec region, the clad temperature shows a closely similar value to the void temperature. Afterward, however, the liquid film dries out and there is almost no difference of void temperature up to C-point where exists an

insulated state. At C-point, there is no cooling effect existing, and temperature rises due to the heating by the fuel.

On the other hand, the clad temperature at the blanket will quickly rises from its original 730°C being heated by the high temperature sodium from the core, and at b-point, where contacting void, no difference of temperature from the clad temperature in the core will any longer exist. Then, at c-point, different from the dried out core section, in the blanket section as there remains liquid film, the temperature there is set under the influence of the void pressure (consequently, by temperature) up to d-point where the said temperature changes approximately in the same manner and degree as that of the void temperature. d-point is the point where the clad is cooled by the cooled reentry sodium liquid column.

As described above, the liquid film is an important element. The change of its thickness by vaporization and condensation is given as follows:

(3) Time dependency of liquid film thickness.

Fig. 6-7 is a plot drawing arranging against time the thickness of liquid film in the respective meshes in the axial direction. In this drawing, although in order to avoid complications, a co-ordinates shaft is shifted in each mesh along the horizontal line. The horizontal lines which indicate time are the same with each other. The numbers in the drawing represent the axial direction liquid film mesh number existing within void. In a channel blockage accident, where the liquid existing under void will hardly move, the mesh point marked with d will be the point where is the first existing film. (1) - (5) in the drawing may be the points to indicate the order of the birth of the liquid films (in other words, where void has passed).

Now then, considering a standard case, as the thickness of the initial liquid film is set to 0.1mm, the film thickness at (1) begins with 0.1mm, and with the lapse of time, although there may be a slight increase or decrease, its thickness may continues to be about 0.1mm up to a 0.025 sec region. Thereafter, the thickness continues to decline until it finally wears out at around a 0.085 sec region. With regard to liquid films of (2), (3), (4) and (5), approximately the similar trend is indicated. The vibration which occurs in the process is considered due to the vibration

caused by the void pressure (refer to Fig. 6-4).

6-2.2. Influence of Parameters.

A survey was previously performed on such parameters which were considered to influence the ejection and reentry. Here, taking a standard case as our target, we will investigate the effect of parameters by changing each of them. As one criterion for making judgement of the degree of influence, we will check on the relation between the position of void boundary face and the time.

(1) Initial super heat.

Fig. 6-8 represents the difference of void position in a case when the degree of initial super-heat Δ Ts is changed to each of 50°C, 100°C and 200°C. The results are obvious. The time lapse required by void to reach the blanket exit when Δ Ts is 200°C is less than one half of the time required when Δ Ts is 50°C. The time required for void to make reentry into the blanket is 40m/sec when the super-heat is 200°C, while it is only 20m/sec at 50°C. Thus, there is a tendency that a higher super-heat takes a longer reentry time. But once a reentry is started, the time requirement until the reentry is completed (time from the commencement of the liquid column entry into the blanket until the bubble collapse and disappear) is 25m/sec at Δ Ts = 200°C, while it is 35m/sec at Δ Ts = 50°C, thus showing a tendency that the larger is Δ Ts, the faster is the time.

It is also known that the highest point, to which the void end-face ascends inside the sodium plenum at the upper section of the blanket which is hypothetically provided, is higher as the super-heat is larger.

The driving force of the liquid column movement is the vapor pressure, of which general picture has been given in Fig. 6-4. Therefore, here, Fig. 6-9 represents the Δ Ts of the initial stage (μ sec order) and the influence of the condensation coefficient value C as described below. By the drawing, it is noticed how big is the effect of Δ Ts. The dot-chained line in the drawing indicates the saturation pressure against the sodium temperature at the time of boiling by adding the excess heating degree to the saturation temperature. That is, if the phenomenon is slow and gradual, then as it is to show the pressure upon this dot-chained line, it may be said that the difference between the pressure value calculated

hereby and the dot-chained line represents the degree of a sudden boiling.

The effect of the condensation coefficient C is substantially large so long as time is extremely short (about 10^{-15} sec), but afterward, having saturated with $\triangle$ Ts features, the difference becomes conspicuous. Furthermore, during the initial 10^{-5} sec, it does not necessarily influence the phenomenon because of the force of inertia. The next drawing shows the effect of C as a proof of this fact.

(2). Condensation coefficient.

Fig. 6-10 indicates the difference of C value when taken at 0.1 and 0.5 respectively, of which result can be said nearly correct. Particularly at the initial stage of ejection, it is in a complete concordance. In the latter part of ejection and at the time of its reentry, the size of the condensation coefficient has a great bearing, and the resulting differences are as shown in the drawing.

(3) Initial liquid film thickness.

Fig. 6-11 shows how will affect the difference of thickness of liquid film. Liquid film is regarded as the source of vaporization. Therefore, if there is no liquid film, the growth of void can be controled or prevented. In this sense, if a liquid film can be dried out at its early stage, a change may be brought upon a phenomenon. As indicated in Fig. 6-7, it is after 0.85 sec (at 0.1mm thickness) that liquid film dries out. Whereas, if there is any effect wrought upon, it must be after that. The drawing obviously indicates this fact. The thicker is the liquid film, the slower is the drop of void pressure, and consequently the reentry time also delays.

(4). Heat generation rate at the blanket section.

It is considered that in case the heat generation rate at the blanket section changes, the axial direction temperature distribution of the sodium immediately prior to boiling and of the cladding also will change, and will affect the void growth.

Fig. 6-12 figures out the difference of void position in case when the blanket power is changed to 0.07, 0.14, and 0.21 KW/cm. Generally, the blanket section has a lower temperature prior to boiling than in the

core, and the void partially condenses at the blanket section. If the blanket power is high and the clad temperature prior to boiling is also high, the condensation capacity becomes smaller and the hampering effect upon void growth reduces. The drawing clearly indicates this fact, but the effect is not so large.

(5) Space mesh number.

As this code is seeking the numerical keys by a method of finite difference of a momentum energy equation, it is necessary to examine that the mesh number does not affect the keys.

Fig. 6-13 is the result obtained by doubling the mesh number (10 at the core and 4 at the blanket upper section) in a standard case and compared against those of a standard case. The reason for the time lag of boil commencement is because the positioning is determined by the mesh loop, while as the difference of ejection time is because of the time lag of boil commencement, it is not necessarily an essential element, and it may be said the concordance is satisfactory. But with respect to reentry, there is observed a substantial discrepancy, which may pose some future problems.

(6) Size of boiling nucleus

The size of the initial void was compared with 10^{-4} and 10^{-3} (m) values as it was feared to be affected by the void pressure change in the early stage of boiling. There however, no effect by void position was seen. This may be because of the same reason that the size of the condensation coefficient has no much effect due to the early boiling stage. That is, it may be that the degree of void pressure in its early stage (of 10^{-6} sec order) has no appreciable effect due to the influence of the inertia of liquid.

6-2.3. Boiling Arising from Pumping Trouble.

The phenomenon of flow deterioration and subsequent boiling arising as the result of a channel entrance blockage has been analized in the chapters of 6-2.1 and 6-2.2. In this case, void has not grown up in the lower part of the channel due to the effect of the channel entrance

blockage and by the effect of the pressure at the channel entrance being maintained at its rated capacity. As the result, the reentry is seen being made only from the upper section.

In the case where the channel entrance pressure is approximately equivalent to the pressure at the channel exit, and when there is no blocking obstruction, void is expected to grow at both the upper and the lower sections. The trouble in the case may be such ones, for instance, as a slow-down of flow possibly caused by a pump trip. That is, by some reasons, if a pump loses its pumping pressure by certain constant time number, the pressure at the channel entrance is considered to lose the same certain time constant.

Here, in the case that the certain time constant τ of the pressure decrease is 1.0 sec and also with respect to the case of 0.1 sec, an analysis of boiling phenomenon was conducted. With the decrease of pressure at the channel entrance, the channel flow deteriorates. The calculation with SUSIE-II gives the function of pressure decrease and the subsequent flow deterioration by the following equations:

$$P_{inlet} = (P_1 - P_2)e^{-t/\tau} + P_2 \qquad (6\text{-}5)$$

$$W = \left\{ (P_1 - P_2 - \rho hg) * (2*D\rho S^2)/\lambda h \right\}^{1/2} \qquad (6\text{-}6)$$

Where, P_{inlet} : Pressure at channel inlet (Kg/m^2)

P_1: Pressure at channel inlet under normal condition (Kg/cm^2)

P_2: Pressure at channel outlet under normal condition (Kg/cm^2)

τ: Time constant of cost down (sec)

ρ: Average density of sodium ($Kg*/cm^3$)

g: Acceleration of gravity (m/h^2)

D: Equivalent diameter of channel (m)

S: Channel cross section (m^2)

h: Channel length (m)

λ: Channel pressure drop coefficient

The calculation result is given in Fig. 6-14. In the case of τ = 1.0 sec, the flow volume is about 20% at the time of boil commencement, and partly due to the influence of inertia of a fluid, void does not grow in the lower part, instead it goes into the blanket region and collapses and disappears.

In the case of τ = 0.1 sec, at the time of the boil commencement, the fluid has become almost zero, and the pressures at both the entrance and the exit of the channel are nearly the same. As seen from Fig. 6-13, the void is vibrating, and after once passing through from the lower part, it vanishes at about 0.4 sec after the boiling has commenced. The calculation results of τ = 0.1 sec and of a channel blockage accident are compared in Fig. 6-15. From this comparison, the following matters are made clear:

i) The void occurring points are all nearly the same.

ii) During the blocking of channel, the void growth is only in the upper section. But when pressure decreases, it happens in both the upper and the lower sections.

iii) The life of a single void under a pressure drop is about three times as long as that in the case of a channel blocking.

The above mentioned phenomena of ii) and iii) have a correlational relation. Namely, as voids do not grow in the lower section in the case of a channel blockage, the ratio of the hot zone in the core section out of the void region reduces as void becoming larger. By the time when a reentry begins, a part of the core has already been dried out. Consequently, no sufficient heat generation rate can be obtained to produce and grow voids again, and therby voids vanish in practically a short time.

On the other hand, in the case of a pressure drop, as void grows in the lower section, the ratio of void in the core section is larger than in the case of a channel blocking, and the vaporization volume becomes larger for that ratio, and thereby, the life of a void, though vibrating, extends further. At any rate, it is hard to consider that such a pressure drop at the channel entrance such as τ = 0.1 sec would occur as a reality of an accident, and rather a case of channel blocking may be considered as more general.

Conclusion

By virtue of SUSIE-II Code which was prepared as the result of the development effort undertaken under contract this time, it was possible that the boiling behaviors inside a single channel including reentry were sought by calculation.

The main items which were known and clarified by this study and experiment are as follows:

(1) In the case of a channel entrance blockage (flow deterioration to 1% of the rated capacity), there occurs without failure a sodium reentry into the core within the scope of the parameters as hereby considered.

(2) In the case of a pressure drop at the channel entrance by, for example, a pump trip trouble, the positions of the upper and the lower end-faces of void vibrate at times, and also it happens that sometimes the void end-face passes through downward.

(3) The typical demonstration of void movement is shown by Fig. 6-3 in the case of a channel blockage accident, and by Fig. 6-14 in the case of a channel entrance pressure drop accident.

(4) The largest phenomenon controling factor is a super heat, and not dependent so heavily upon condensation coefficient. Likewise, the liquid film thickness and the difference of immediate pre-boil temperature distribution also are the causes of substantial effect.

The following may be considered as the future problems:

(1) Handling of voids outside the blanket region affecting and disturbing the reentry timing must be further rearranged and coordinated to match the actual situation.

(2) An appropriate consideration must be provided for the handling of such situation where a bubble, which has once vanished after making a reentry, is reborn and grows at the same position or at other position, and thereby a boiling occurs. In this case, there may arise a problem of stability since there is a possibility of plural number of bubbles (piston type void) being produced.

(3) Further check on various parameters which are used as input must be made so that they will concur with the actual situation.

(4) Evaluation and study of technique and method applicable to the analysis of phenomena of one assembly unit (multichannel) may have to be undertaken.

Words of Appreciation

This code has been developed and prepared as the results of a work performed under contract with Power Reactor and Nuclear Fuel Development Corporation (PNC).

We, the authors, hereby wish to express on this occasion our most sincere appreciation of the advice, assistance and cooperation provided to us all through this development work by the members of the FBR Safety Research Technical Committee, particularly by Messrs. Narihiro An and Shunsuke Kondo of the same Committee.

Also, we wish to thank Messrs. Osamu Kawaguchi and Akira Ohtsubo of the FBR Headquarters of PNC for their positive cooperation in providing us the necessary data for the development of this code.

References

(1) R.M. Singer and R.E. Holtz; On the Role of Inert Gas in Incipient Boiling Liquid Metal Boiling, Int. J. Heat Mass Transfer 12 (1969), pp.1045-1060.

(2) R.E. Holtz and H.K. Fauske; The Prediction of Incipient Boiling Super-heats in Liquid Metal Cooled Reactor Systems, Nuclear Engineering and Design, 16 (1971) pp.253-265.

(3) Edoward and Hoffman; Superheat with Boiling of Alkali Metals, ANL-7100 (1965) p.515.

(4) A.F.Mills and R.A. Seban; The Condensation Coefficient of Water, Int. J. Heat Mass Transfer, 10 (1967), pp.1815-1827.

(5) Pezzilli et al.; The NEMI Model for Sodium Boiling and Its Experimental Basis, ASME 1970, Winter Meeting.

(6) J.M.Kay; Fluid Mechanics and Heat Transfer, Cambridge Press, (1957), p.170.

LIST OF CODES

T	:	Temperature	(^{o}C)
t	:	Time	(h)
C	:	Specific heat	(Kcal/Kg ^{o}C)
k	:	Thermal conductivity	(Kcal/mh ^{o}C)
Q	:	Heat generation rate	(Kcal/m^3 h)
r	:	Radial direction distance	(m)
q_G	:	Gap thermal flux	(Kcal/m^2 h)
h_G	:	Gap conductance	(Kcal/m^2 h ^{o}C)
α	:	Thermal diffusivity	(m^2/h)
Nu	:	Nusselt's number	
Pe	:	Peclet's number	
D	:	Equivalent diameter	(m)
Z	:	Distance from channel entrance	(m)
W	:	Flow rate	(Kg/h)
S	:	Channel cross section	(m^2)
$\dot{n}$	:	Evaporation rate	(Kg/m^2 h)
h_{fg}	:	Evaporation latent heat	(Kcal/Kg)
f_k	:	Condensation coefficient	
R	:	Gas constant	(Kg weight m/mol ^{o}C)
T_f	:	Liquid film surface temperature	(^{o}C)
T_v	:	Void temperature	(^{o}C)
A	:	Sodium weight per mol	(Kg/mol)
N	:	Vapor weight volume inside void	(Kg)
V	:	Void volume	(m^3)
v	:	Moving speed of void boundary face	(m/h)
g	:	Gravity acceleration	(m/h^2)
λ	:	Pressure drop coefficient	
δ	:	Orifice coefficient	(m^{-1})
ℓ	:	Thickness of liquid film	(m)

Table 1-1. Main Differences between SUSIE and SUSIE-II

Items	SUSIE	SUSIE-II
Basic calculation model	Single bubble model	Single bubble model
Accident factors	Channel blockage. Heat generation rate increase .	Channel blockage. Heat generation rate increase. Pressure change at Channel entrance.
Reentry	None	Reentry calculation is possible.
Temperature calculation of film and clad	Each separately calculated for each mesh	Both integrally and averagely calculated. (Film and clad are of the same temperature. only for post-boil calculation)
Time mesh	Cut into certain interval of time	Automatic adjustment wi with the mesh width. (Dependent on void presure change)

Table 5.1 Library

PROPERTIES OF SODIUM

TG(C)	VG(M^3/KG)	PS(ATM)	TG(C)	VG(M3/KG)	PS(ATM)	TG(C)	VG(M3/KG)	PS(ATM)
0.560E+03	0.175E+03	0.183E-01	0.580E+03	0.128E+03	0.231E-01	0.600E+03	0.919E+02	0.322E-01
0.620E+03	0.682E+02	0.442E-01	0.640E+03	0.513E+02	0.599E-01	0.660E+03	0.391E+02	0.861E-01
0.680E+03	0.301E+02	0.106E+00	0.700E+03	0.235E+02	0.138E+00	0.720E+03	0.185E+02	0.178E+00
0.740E+03	0.147E+02	0.227E+00	0.760E+03	0.118E+02	0.285E+00	0.780E+03	0.956E+01	0.361E+00
0.800E+03	0.781E+01	0.448E+00	0.820E+03	0.845E+01	0.552E+00	0.840E+03	0.533E+01	0.676E+00
0.860E+03	0.445E+01	0.821E+00	0.880E+03	0.375E+01	0.987E+00	0.900E+03	0.318E+01	0.118E+01
0.920E+03	0.271E+01	0.140E+01	0.940E+03	0.233E+01	0.185E+01	0.960E+03	0.201E+01	0.194E+01
0.980E+03	0.174E+01	0.227E+01	0.100E+04	0.151E+01	0.264E+01	0.102E+04	0.132E+01	0.305E+01
0.104E+04	0.116E+01	0.351E+01	0.106E+04	0.102E+01	0.503E+01	0.108E+04	0.906E+00	0.460E+01
0.110E+04	0.805E+00	0.525E+01	0.112E+04	0.718E+00	0.592E+01	0.114E+04	0.642E+00	0.668E+01
0.118E+04	0.578E+00	0.751E+01	0.118E+04	0.518E+00	0.842E+01	0.120E+04	0.468E+00	0.941E+01
0.122E+04	0.425E+00	0.105E+02	0.124E+04	0.384E+00	0.118E+02	0.126E+04	0.349E+00	0.129E+02
0.128E+04	0.318E+00	0.142E+02	0.130E+04	0.291E+00	0.157E+02	0.135E+04	0.234E+00	0.198E+02
0.140E+04	0.191E+00	0.245E+02	0.145E+04	0.158E+00	0.301E+02	0.150E+04	0.131E+00	0.364E+02
0.155E+04	0.111E+00	0.438E+02	0.160E+04	0.939E-01	0.517E+02	0.165E+04	0.804E-01	0.607E+02
0.170E+04	0.695E-01	0.707E+02	0.175E+04	0.603E-01	0.817E+02	0.180E+04	0.527E-01	0.937E+02
0.185E+04	0.464E-01	0.107E+03	0.190E+04	0.411E-01	0.121E+03	0.195E+04	0.367E-01	0.136E+03
0.200E+04	0.329E-01	0.152E+03	0.205E+04	0.296E-01	0.170E+03	0.210E+04	0.268E-01	0.188E+03
0.215E+04	0.244E-01	0.207E+03	0.220E+04	0.223E-01	0.228E+03	0.225E+04	0.205E-01	0.249E+03
0.230E+04	0.189E-01	0.272E+03	0.235E+04	0.174E-01	0.295E+03	0.240E+04	0.162E-01	0.320E+03
0.245E+04	0.151E-01	0.345E+03	0.250E+04	0.141E-01	0.371E+03			

Table 5-2. Input Format of SUSIE-II (1)

TITLE 1)	10x,14A5

1) Title

RFUEL 2)	RCLDF 3)	RCLDL 4)	DLIQI 5)	10x, 6E10.3

2) Fuel radius (m). 3) Clad inner radius (m). 4) Clad outer radius (m).

MFUEL 6)	MCLD 7)	MLIQ 8)	10x,6I10

6) Fuel's radial direction mesh number 7) Clad's radial direction mesh number.
8) Film's radius direction mesh number.

MZME 9)	10x,6I10

9) Axial direction region number.

ZREG(I) 10)	I=1, MZME					10x, 6E10.3

10) Axial direction length of region (m)

MZRE(I) 11)	I=1, MZME					10x,6I10

11) Mesh capacity of region ((kW/cm)

PINPH 12)	10x, 6E10.3

12) Distance between pins (m)

HEATPH(I) 13)	HEATPL(I) 14)	HEATAA(I) 15)	10x, 6E10.3

13) Maximum capacity of region I (kW/cm)

14) Location of maximum output in region I (Distance from the channel entrance) (m)

15) Coefficient of output distribution in region I

Note: Output is given by equation.

| THODEM 1) | DENFR 2) |

10x, 6E10.3

1) Theoretical density of fuel (Kg/m^3). 2) Ratio against theoretical fuel density

| TEMNAL 3) | PRESI 4) | PRES2 5) |

10x, 6E10.3

3) Temperature at channel entrance (°C). 4) Pressure at channel entrance (Kg weight/m^2)
5) Pressure at channel exit (Kg weight/m^2)

| FLOW 6) | ARAMI 7) | HFACL 8) |

10x, 6E10.3

6) Channel flow volume (Kg/h). 7) Channel pressure loss coefficient
8) Fuel and clad gap conductance (Kcal/m^2 h °C)

| SPHEAT 9) | CPI 19) | CP4 11) |

10x, 6E10.3

9) Super-heat (°C). 10) Condensation coefficient. 11) Initial bubble diameter (m).

| DTIME 12) | TMAX 13) | EPS 14) |

10x, 6E10.3

12) Time mesh width (sec) 13) Calculation stop time (sec). 14) Accuracy of constant value checking and calculation

| ISKIT 15) | ITIMEM 16) |

10x,6I10

15) Time mesh skip of output. 16) Breakdown of time mesh at initial boiling.

| NVRVL 17) |

8x,I2, 7E10.3

17) Types of accident and trouble.

| INVRVL 18) | VRVL(I) 19) | I=1,7 | | | | | |

8x,I2, 7E10.3

18) Pattern of accident function. 19) Coefficient of equivalent pressure function.

Note: Output is given by equation.

Table 5.3 Example of Input Data

```
 MONJU-2  SAFETY  ANALYSIS          PUMP TRIP ACCIDENT          FEB. 21. 1972
  0.270E-02  0.250E-02  0.315E-02  0.100E-03
         10          3          2
          3          0
  0.356E+00  0.900E+00  0.550E+00
          4         10          4
  0.790E-02
  0.700E-01  0.350E+00  0.100E+00
  0.402E+00  0.800E+00  0.216E+01
  0.700E-01  0.125E+01  0.100E+00
  0.110E+05  0.850E+00
  0.390E+03  0.374E+05  0.154E+05
  0.379E+03  0.0        0.732E+04
  0.500E+02  0.100E+00  0.100E-05
  0.100E-02  0.100E+02  0.100E-01
         50       1000
2
0 0.334E+00  0.0        0.0        0.0       0.0       0.0       0.0
```

Table 5-4. Accident Types and Their Functions

NVRVL	Types	INVRVL	Function
1	Flow decrease (By channel blockage)	0	
		1	f represents flow variation rate
2	Pressure change at entrance	0	P_1, P_2 represent the initial pressure at entrance and exit
3	Orifice diameter change at channel entrance		
4	Heat generation rate change *	0	h represents heat generation rate change

* When reaction feedback or a scram is considered, NVRVL shall be applied with a number of two figures.
The presently applicable ones are the followings:

NVRVL	INVRVL	Function
42	0	$P = (P_1-P_2)e^{-VRVL(1)*t} + 2$ After commencement of boil, scram works at VRVL(3) sec. $h = e^{-VRVL(4)*t}$

Table 5.5 Example of Output

```
SEC= 0.860E-02
     Z1,Z2,W1,W2,DZ
     PGAS,TGAS,NGAS    0.187E+05   0.950E+03   0.458E-07
     LOW TLQD            950.019     936.739     936.150     907.072     905.027     862.661     858.454     805.339     798.351
     LOW TLQD            727.327     656.591     642.536     498.636     404.110     460.583     459.799     455.449     454.810
     LOW TLQD            446.413     393.708
     UP  TLQD            950.578     948.047     948.025     929.043     928.850     895.652     894.449     747.565     738.481
     UP TLQD             726.368     729.933     730.077     733.943     727.598
     TFUEL CENTER        558.985     564.875     570.125     575.551    1283.984    1575.135    1842.615    2048.649    2179.201
     TFUEL CENTER       2180.797    2654.808    1858.403    1611.599     865.324     869.595     874.176     878.756
     TFUEL SURFACE       485.843     492.922     497.914     501.948     797.415     913.267    1011.305    1090.088    1145.183
     TFUEL SURFACE      1182.415    1161.859     114.912    1048.635     774.679     765.055     768.208     776.409
     TCLAD               449.063     457.297     462.416     465.838     654.369     741.919     816.202     870.908     927.238
     TCLAD               974.393     972.261     949.988     916.316     746.431     729.869     732.424     743.427
     TFILM               950.578     950.019     950.578
     SFILM              0.983E-04   0.160E+13   0.161E+13
     QFILM              0.110E+07   0.165E+07   0.110E+07

SEC= 0.860E-02     1= 4301                     TIME= 0731E+00
     Z1,Z2,W1,W2,DZ       0.937       0.942       0.057       1.364   0.574E-02
     PGAS,TGAS,NGAS    0.187E+05   0.950E+03   0.458E-07
     LOW TLQD            950.019     936.739     936.150     907.072     905.027     862.661     858.454     805.334     798.391
     LOW TLQD            446.419     393.708
     UP  TLQD            950.578     948.047     948.025     929.048     928.850     895.652     894.449     747.565     738.481
     UP  TLQD            726.868     729.933     730.077     733.943     727.598
     TFUEL CENTER        559.060     564.898     570.146     575.573    1284.617    1579.163    1842.839    2098.669    2179.219
     TFUEL CENTER       2160.814    2654.826    1858.422    1611.620     865.340     869.609     874.188     878.769
     TFUEL SURFACE       485.857     492.566     497.930     501.963     797.466     913.335    1011.383    1090.174    1146.273
     TFUEL SURFACE      1182.904    1161.948    1114.988    1048.703     774.707     765.072     768.223     776.430
     TCLAD               449.065     457.297     462.416     465.839     654.370     741.925     816.208     878.919     927.250
     TCLAD               974.405     972.274     949.994     916.324     746.431     729.809     732.424     743.427
     TFILM               950.578     950.019     956.578
     SFILM              0.983E-04   0.160E+13   0.161E+13
     OFILM              0.110E+07   0.165E+07   0.110E+07
```

Table 6-1. Input Data for MONJU

Radial direction mesh	Fuel (10), Clad (3), Film (2)
Axial direction mesh	Lower part of blanket (5) Fuel (10), Upper part of blanket (5)
Pin pitch	0.00790 m
Fuel density	Theroretical density (1.10 x 10^4 kg/cm^3) x 0.87
Channel entrance temperature	390.0°C
Channel entrance pressure	4.12 x 10^4 kg/cm^2
Channel exit pressure	1.0 x 10^4 kg/cm^2
Channel flow volume	3.76 x 10^2 Kg/h
Gap conductance	7.33 x 10^3 Kcal/m^2 h
Super-heat	50°C
Condensation coefficient	0.1
Initial bubble radius	1.0 x 10^{-4} m

Table 6.2 Parameters

Case	△Ts	S	C	r	Qb	MZ	Ref Dwgs
Unit	°C	mm		mm	Kw/cm		
Standard	50	0.1	0.1	0.1	0.07	In-core 10 / up Blnkt sec 4	6.3
Super-heat effect	100	*	*	*	*	*	6.8
	200	*	*	*	*	*	
Film thickness effect	*	0.3	*	*	*	*	6.11
	*	0.5	*	*	*	*	
Condensation coefficient	*	*	0.5	*	*	*	6.10
Size of boiling nucleus	*	*	*	1	*	*	-
Heat generation rate blanket	*	*	*	*	0.14	*	6.12
	*	*	*	*	0.21	*	
Axial direction mesh number	*	*	*	*	*	20.8	6.13

Note: * Indicates the same values as those of the standard case

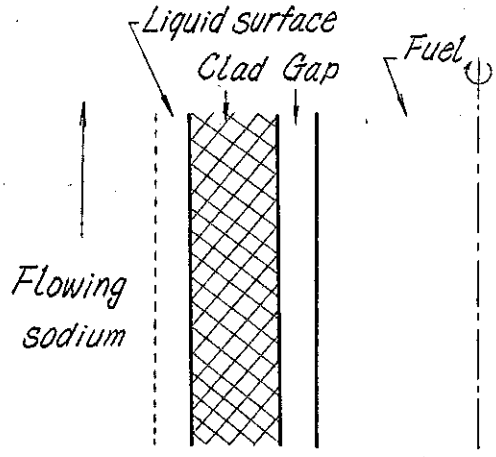

Fig. 1.1. Model of calculation of temperature distribution in fuel and clad.

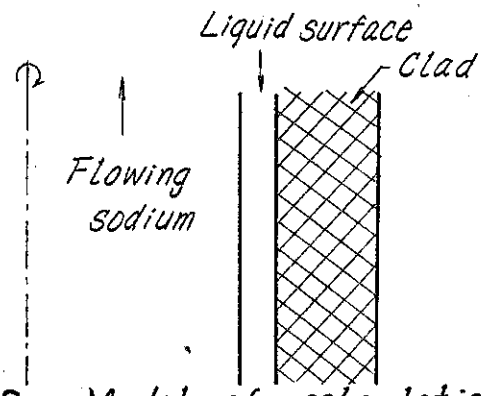

Fig. 1.2. Model of calculation of temperature distribution in flowing sodium.

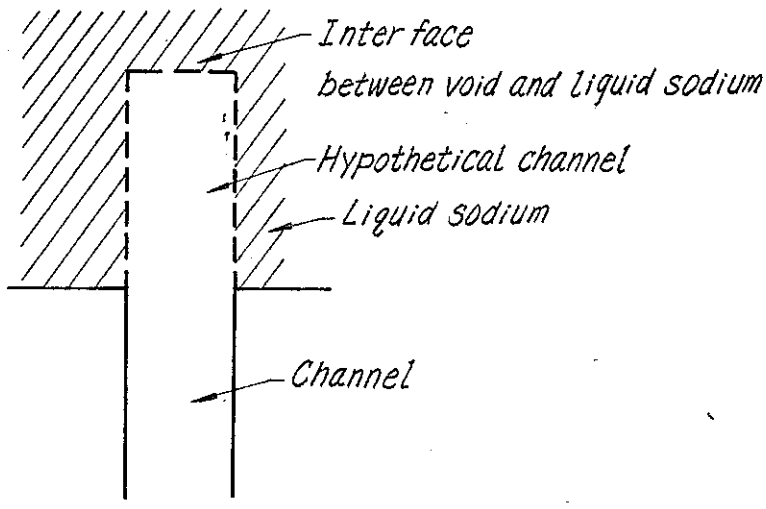

Fig. 1.3. Model of boundary surface between void and sodium outside the channel.

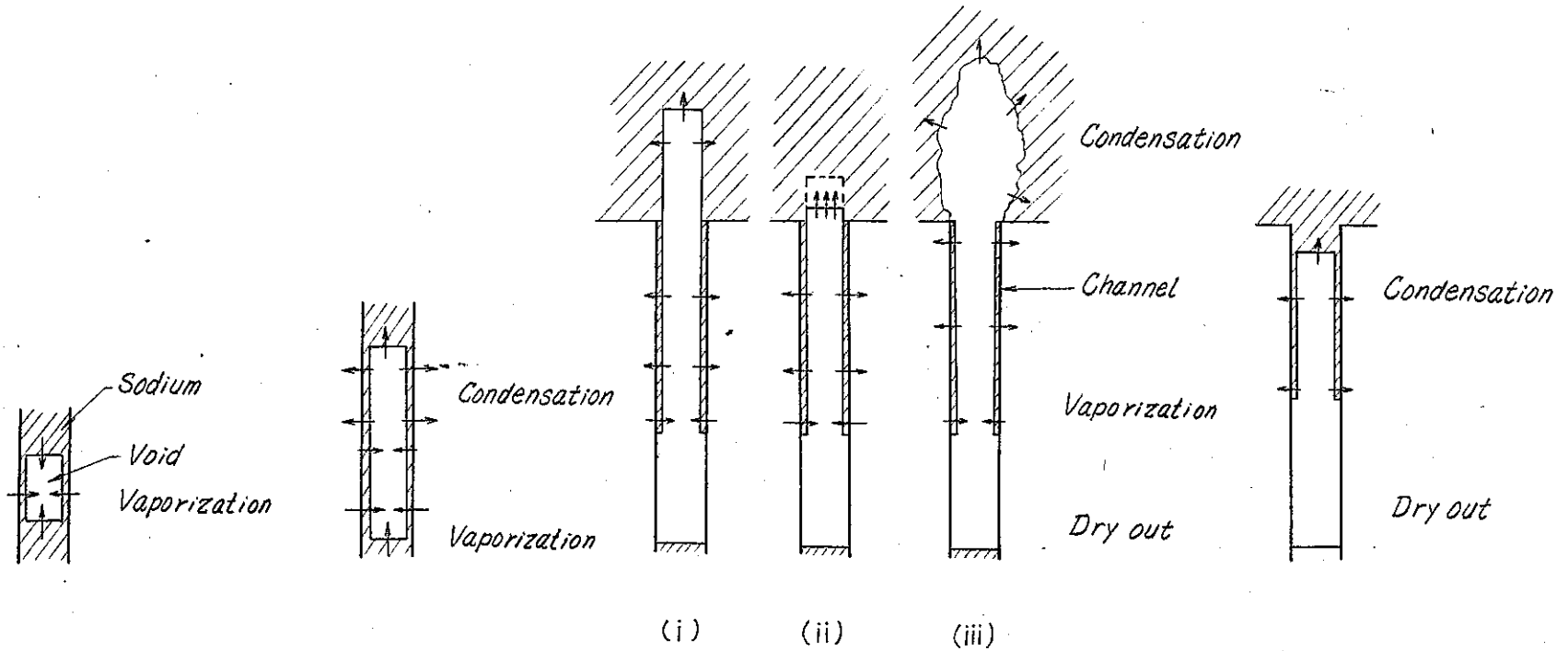

Fig. 2.1 Model of vaporization and condensation in void.

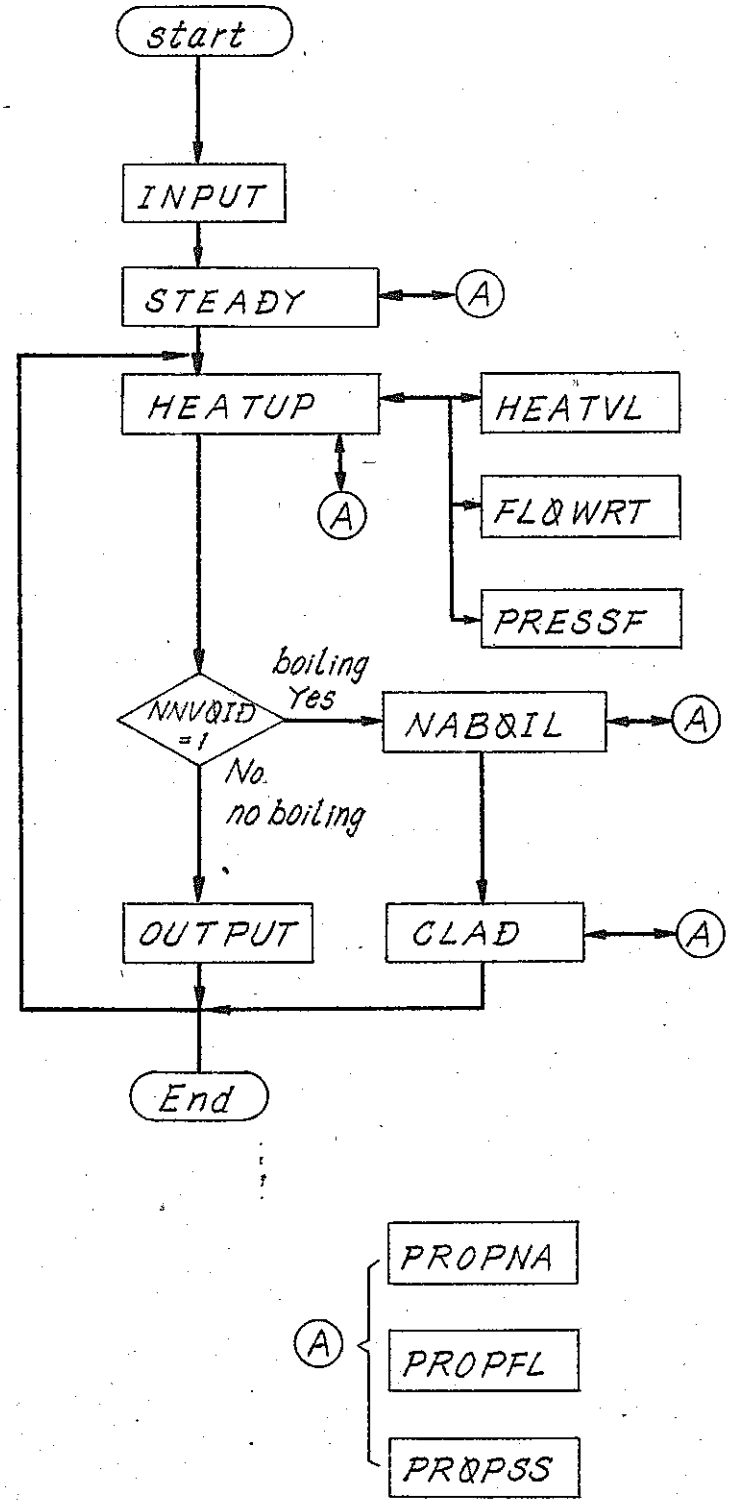

Fig. 4.1. Block diagram of SUSIE - II

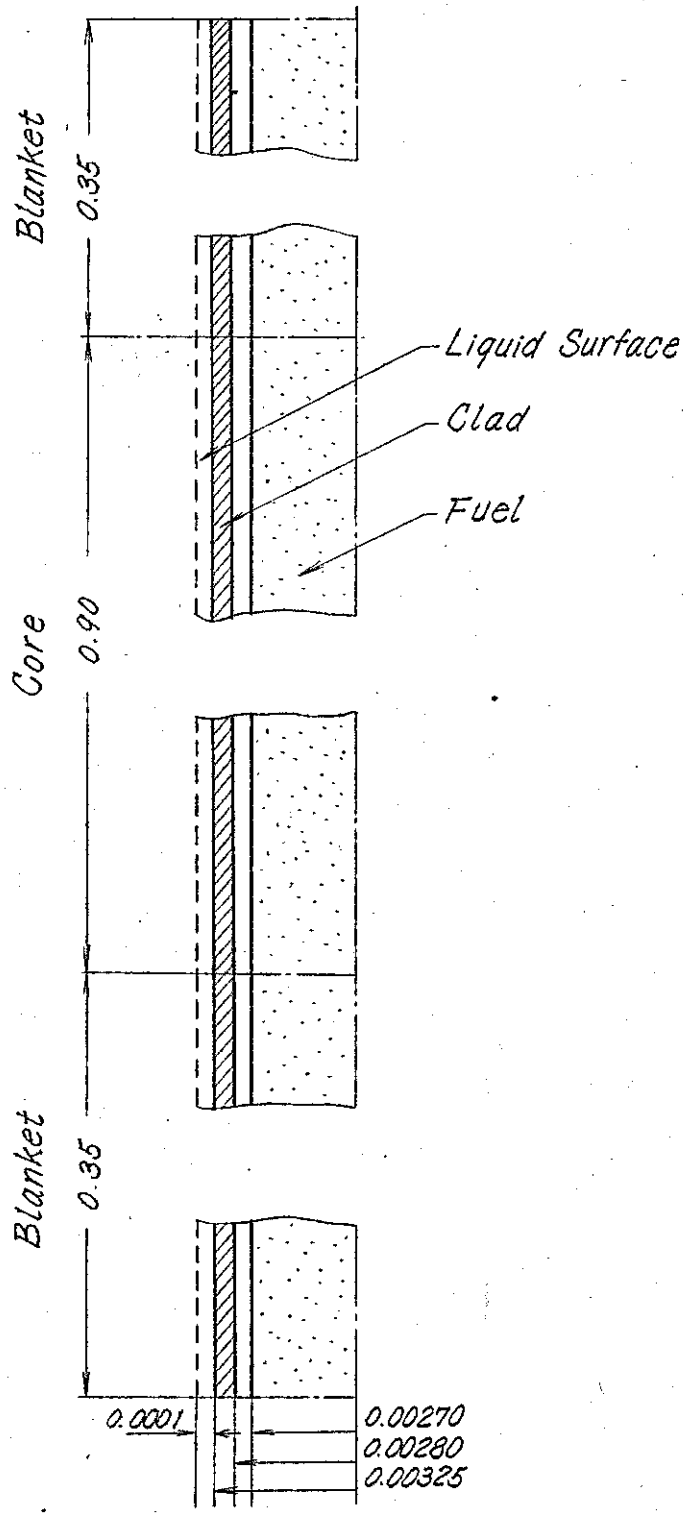

Fig. 6.1. Dimension of fuel and channel.

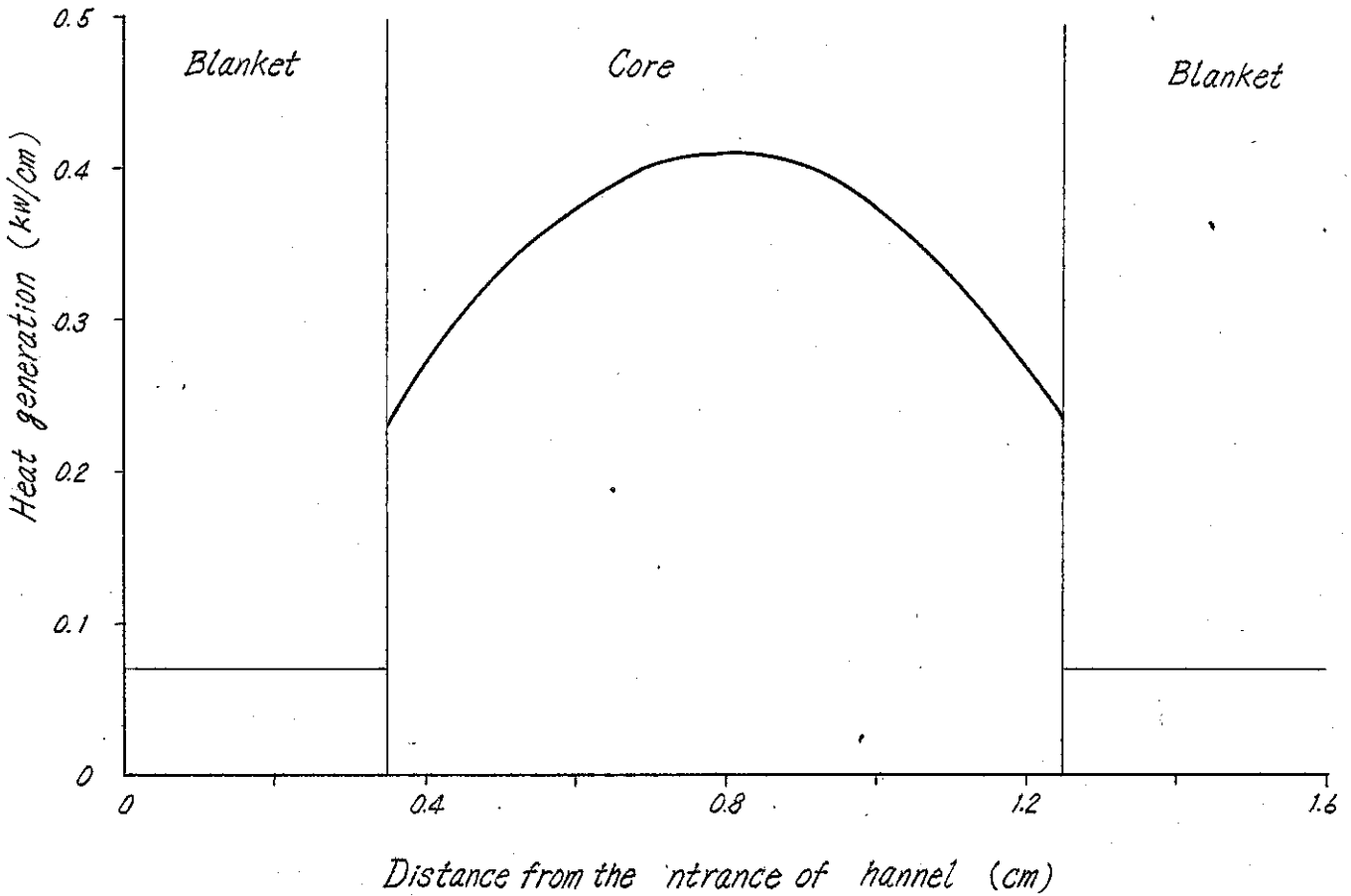

Fig. 6.2. Distribution of heat generation in fuel.

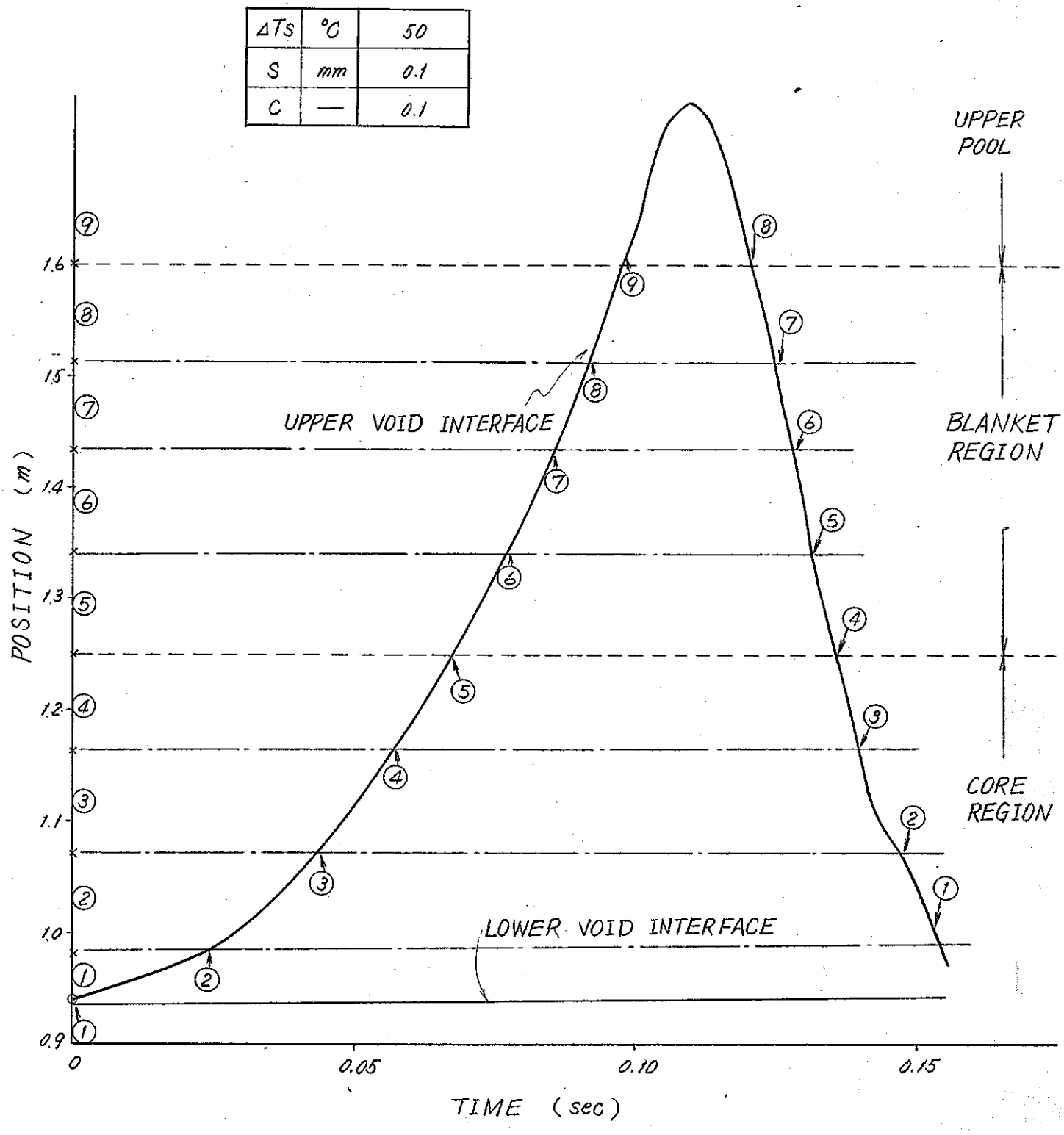

Fig. 6.3. Time dependence of void interface position.

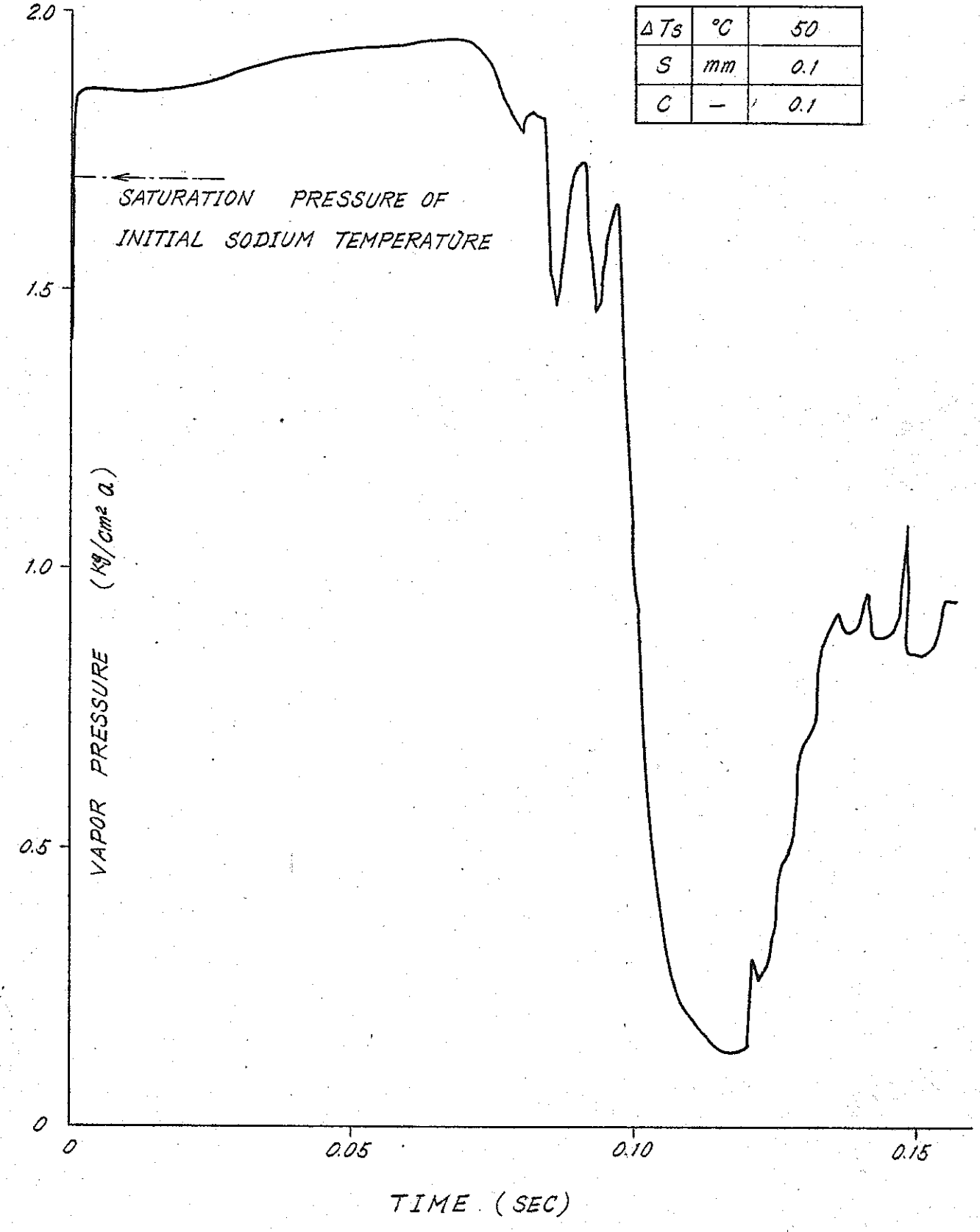

Fig. 6.4. Time dependence of void vapor pressure.

CASE	ΔTs	C	S
BASIC	50	0.1	0.1

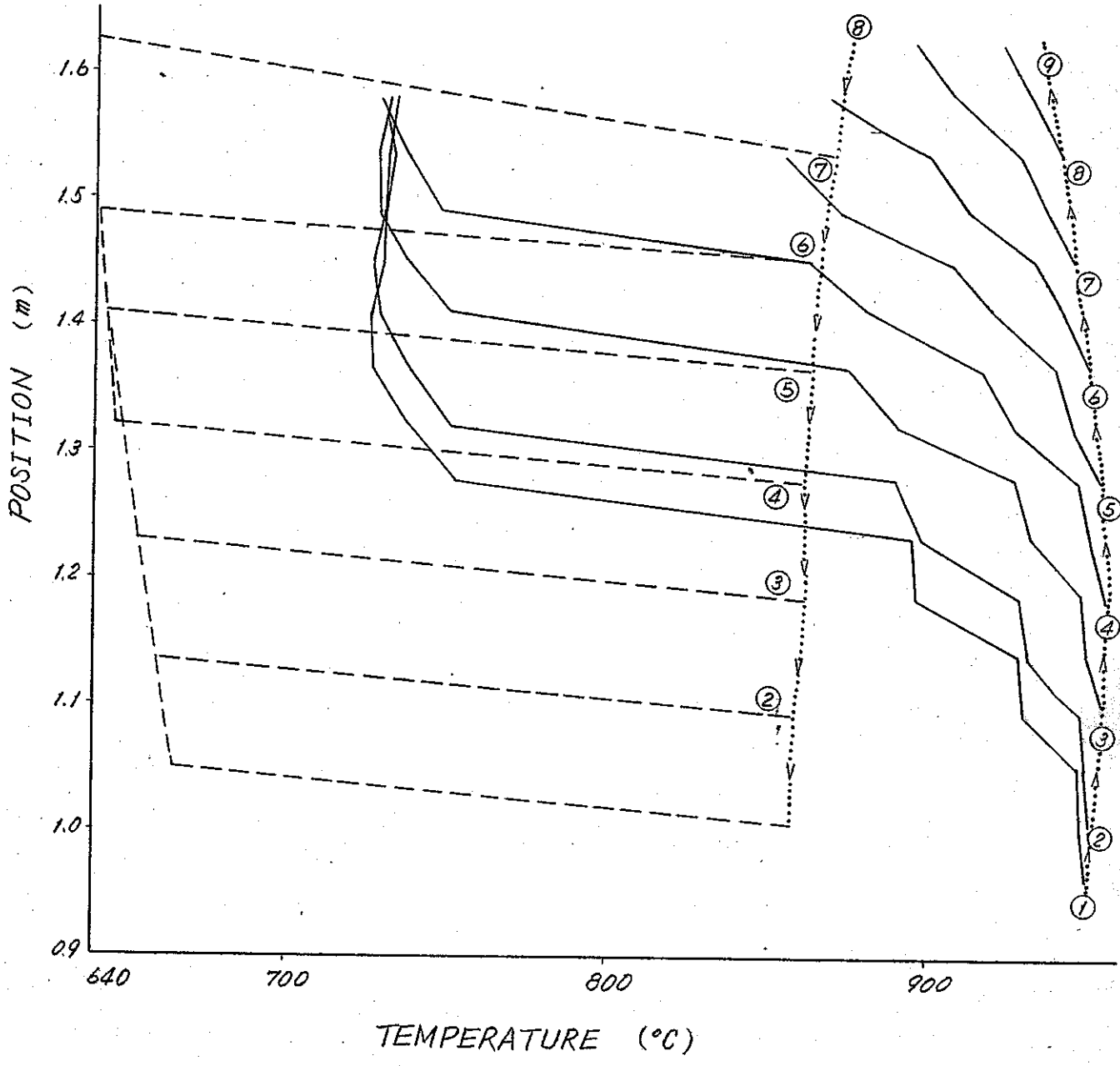

Fig. 6.5. *Time dependence of liquid column temperature.*

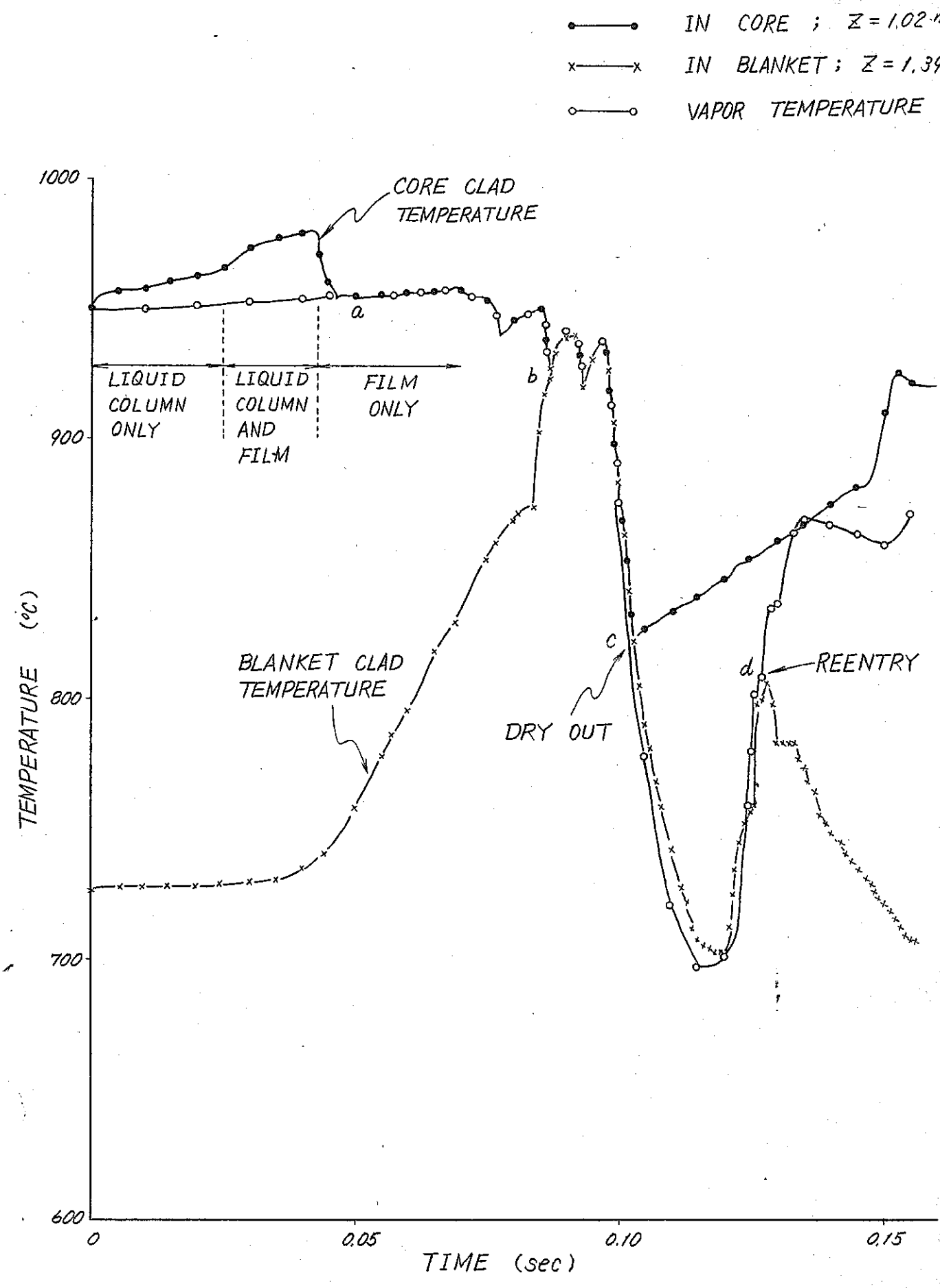

Fig. 6.6. *Time dependence of clad temperature.*

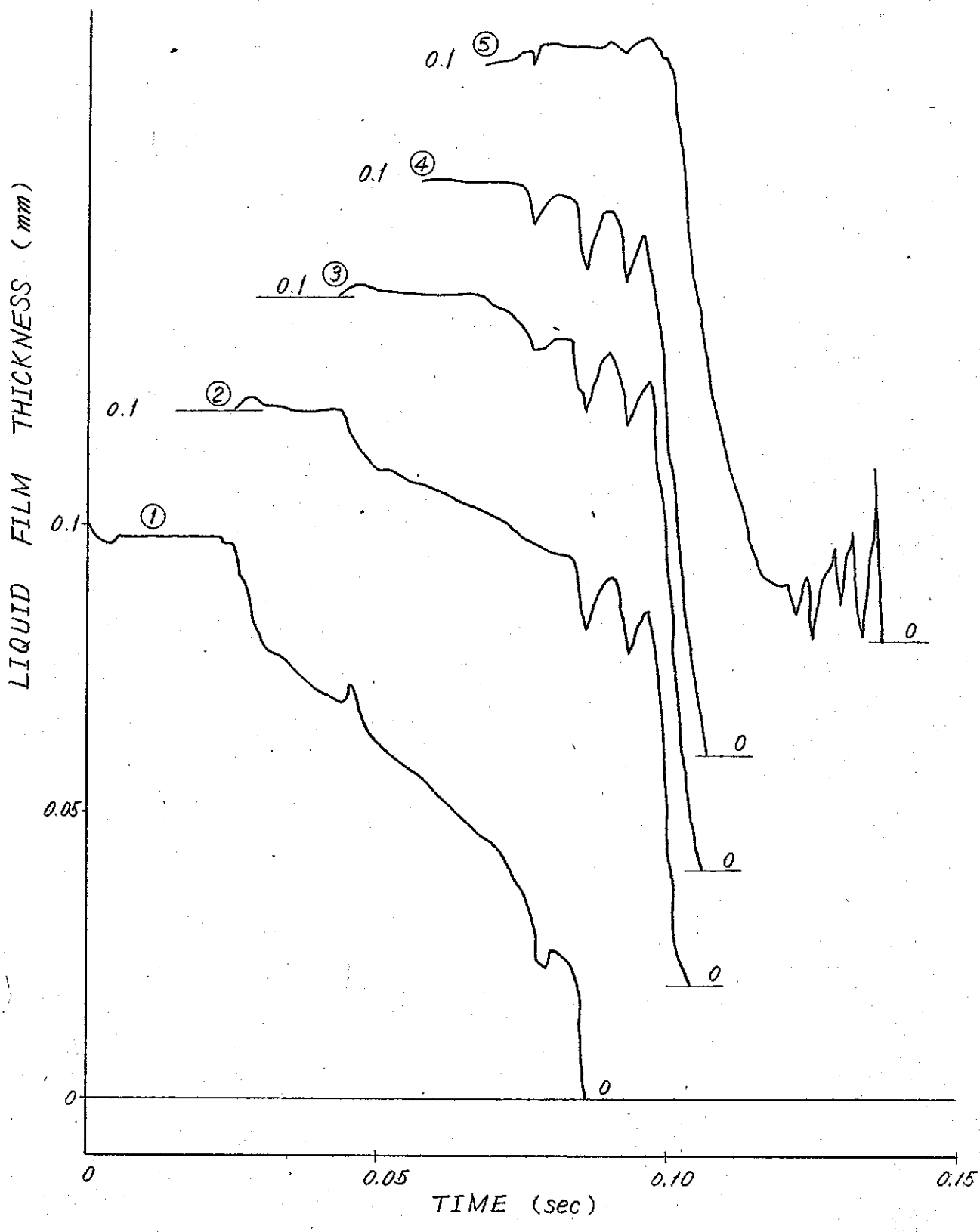

Fig. 6.7. *Time dependence of film thickness.*

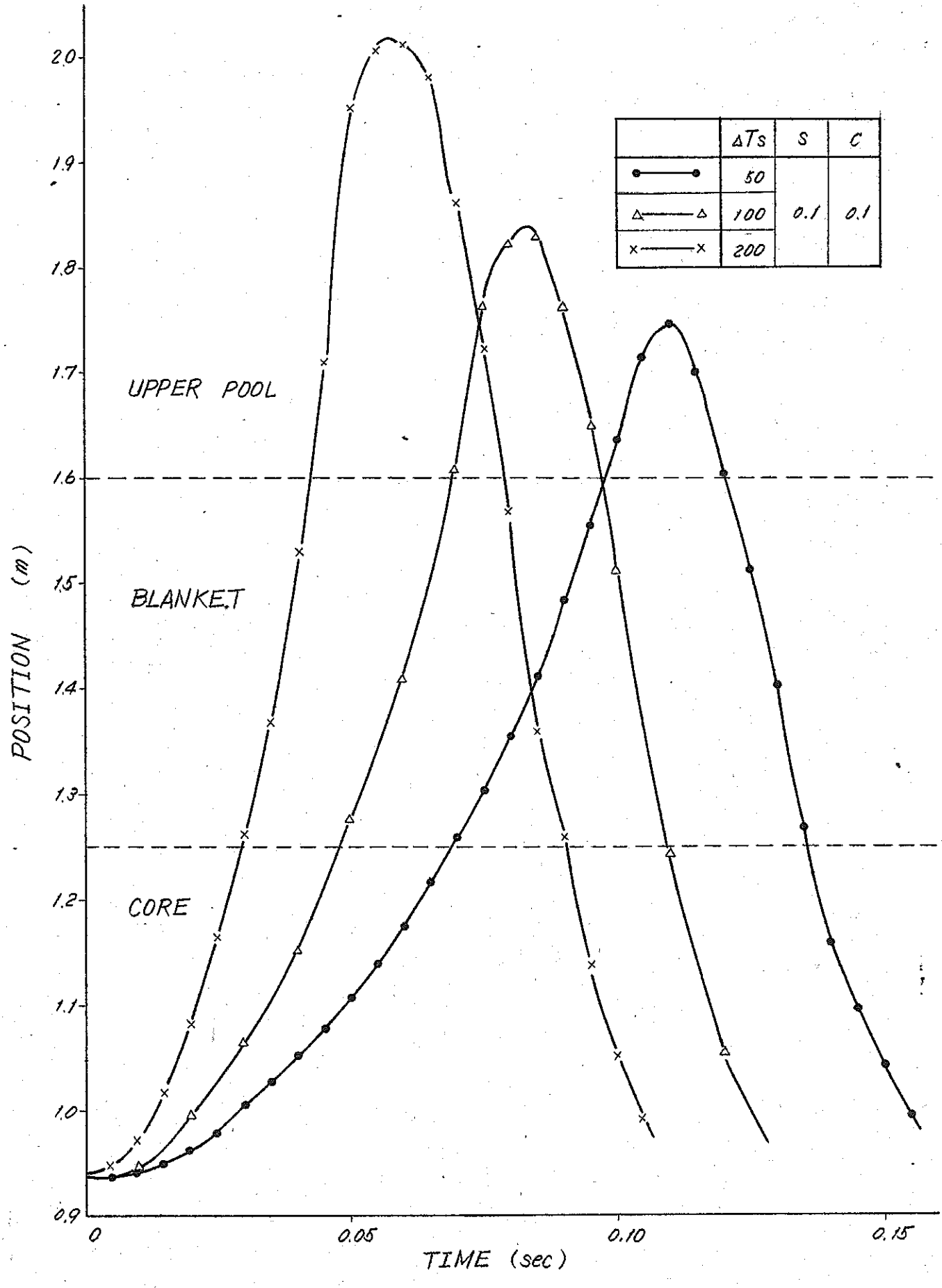

Fig. 6.8. *Effect of superheat on void position.*

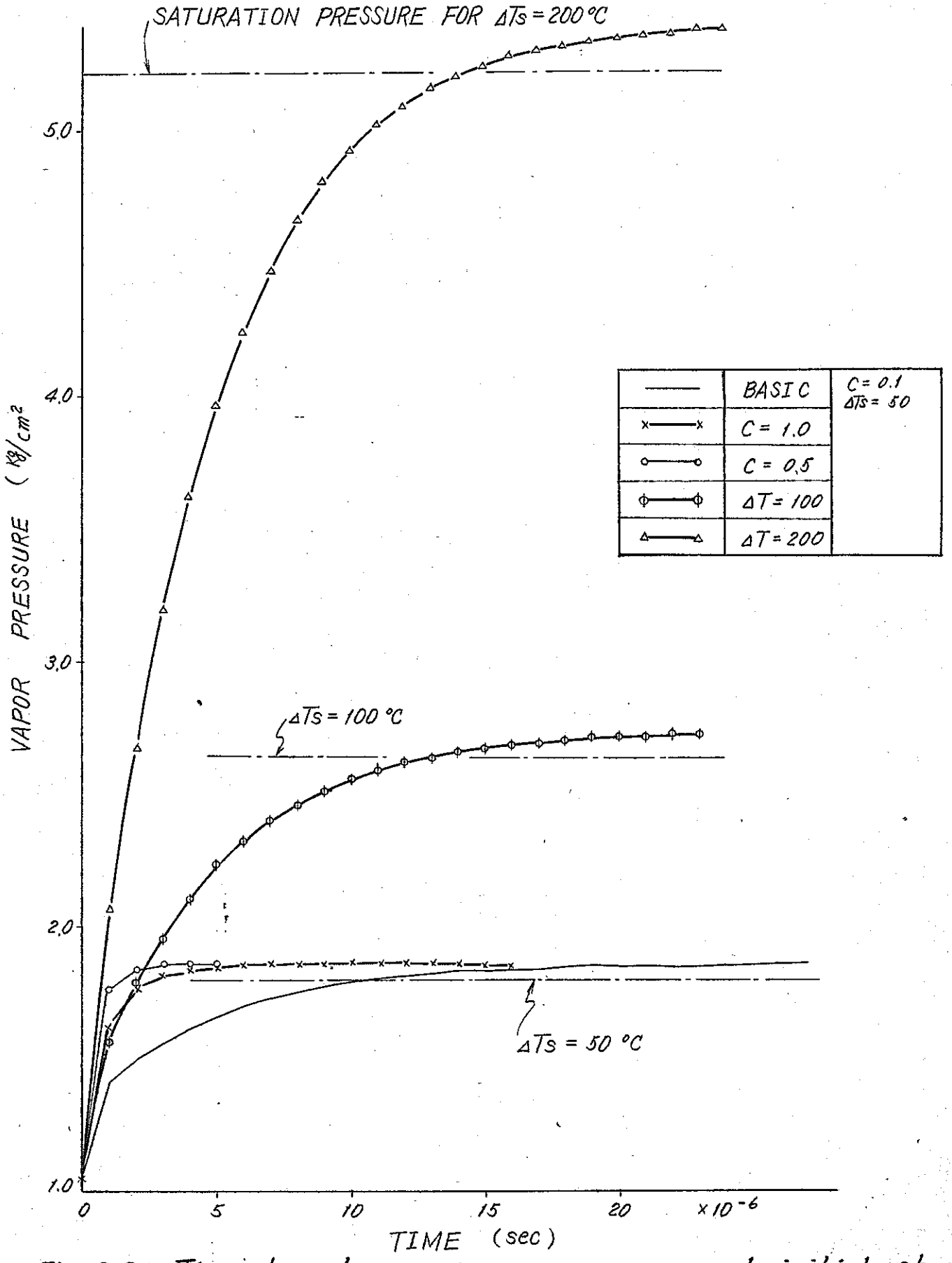

Fig 6.9. Time dependence of vapor pressure at initial stage.

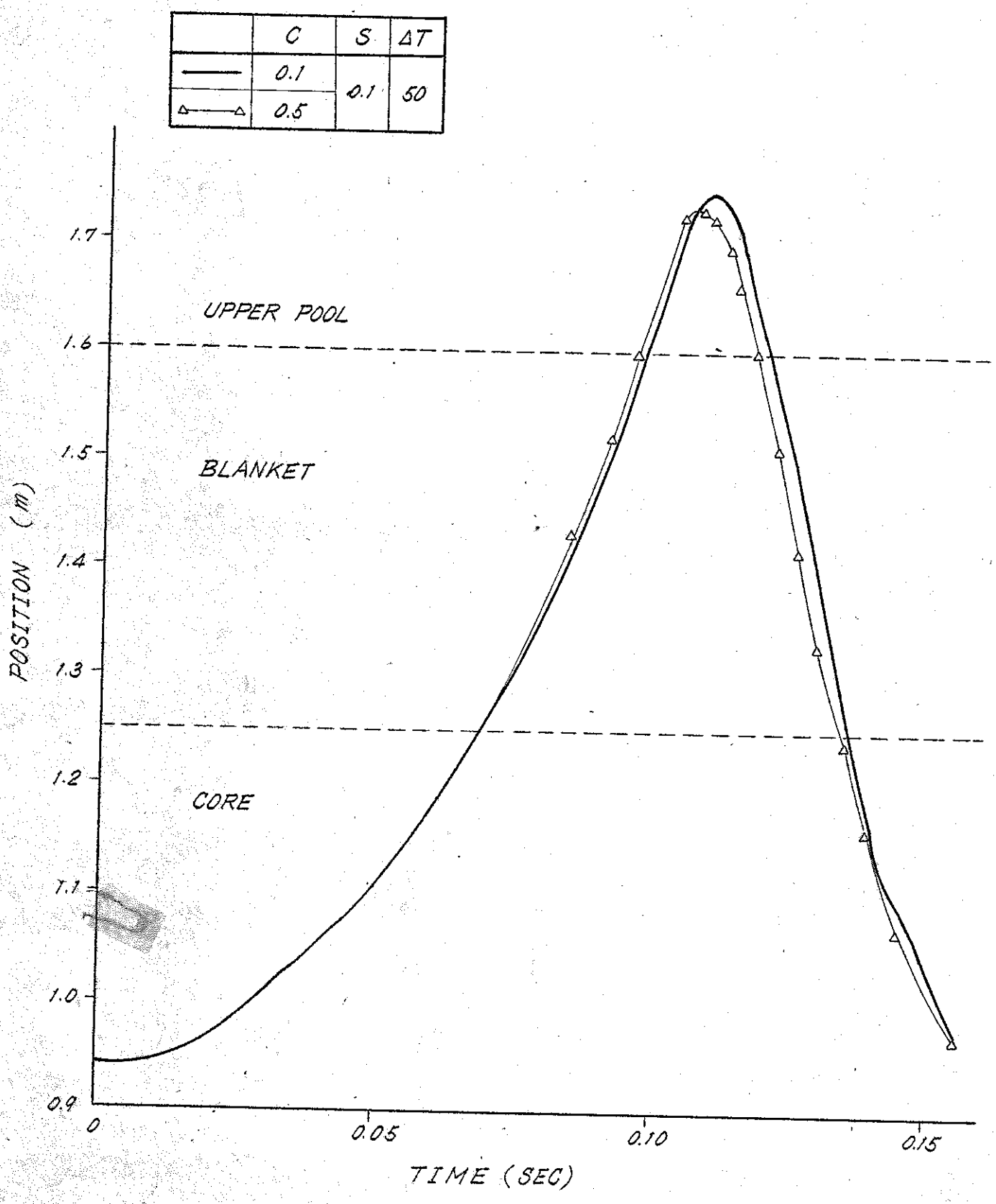

Fig. 6.10. *Effect of condensation coefficient on void position.*

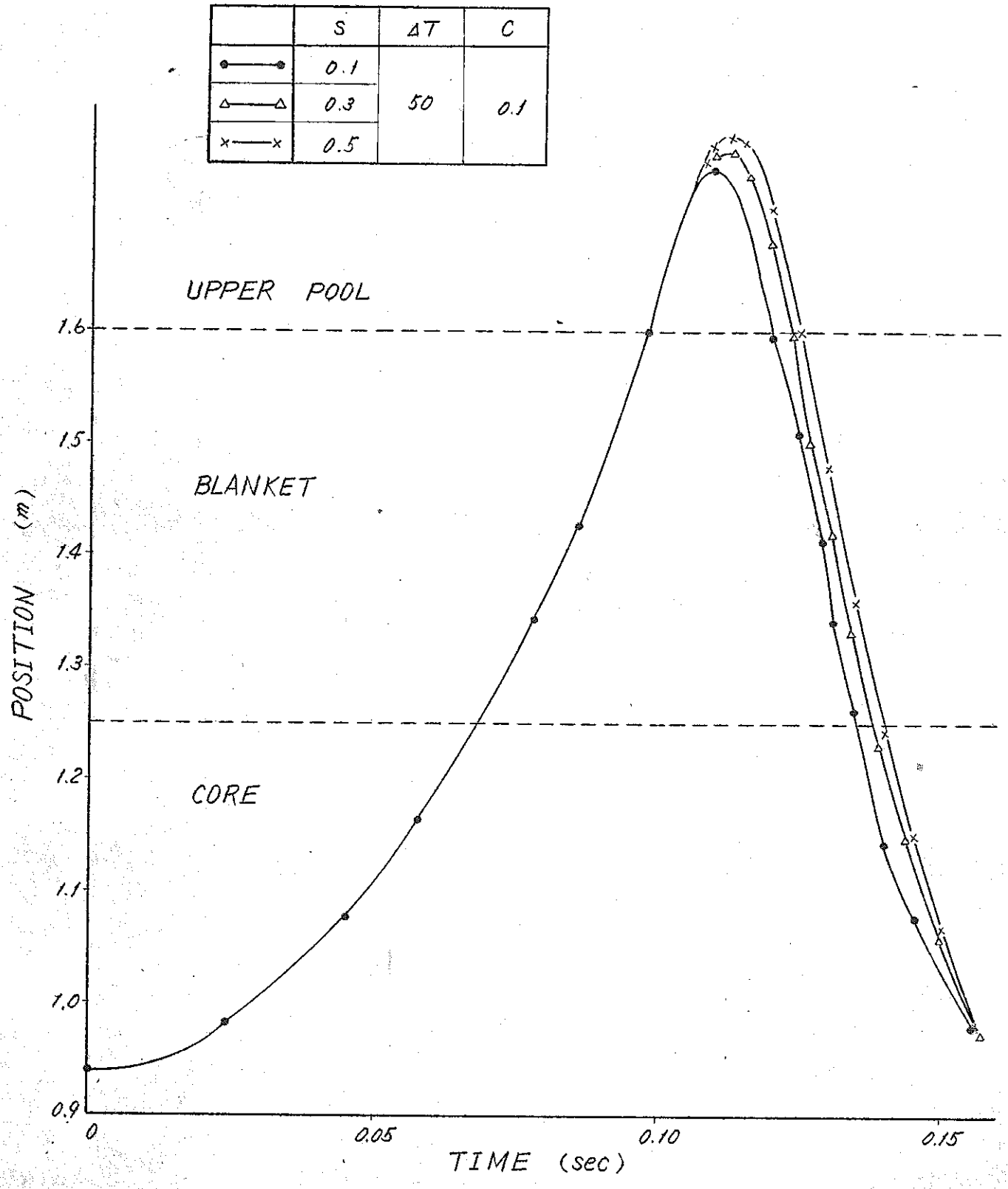

Fig. 6.11. Effect of initial film thickness on void position.

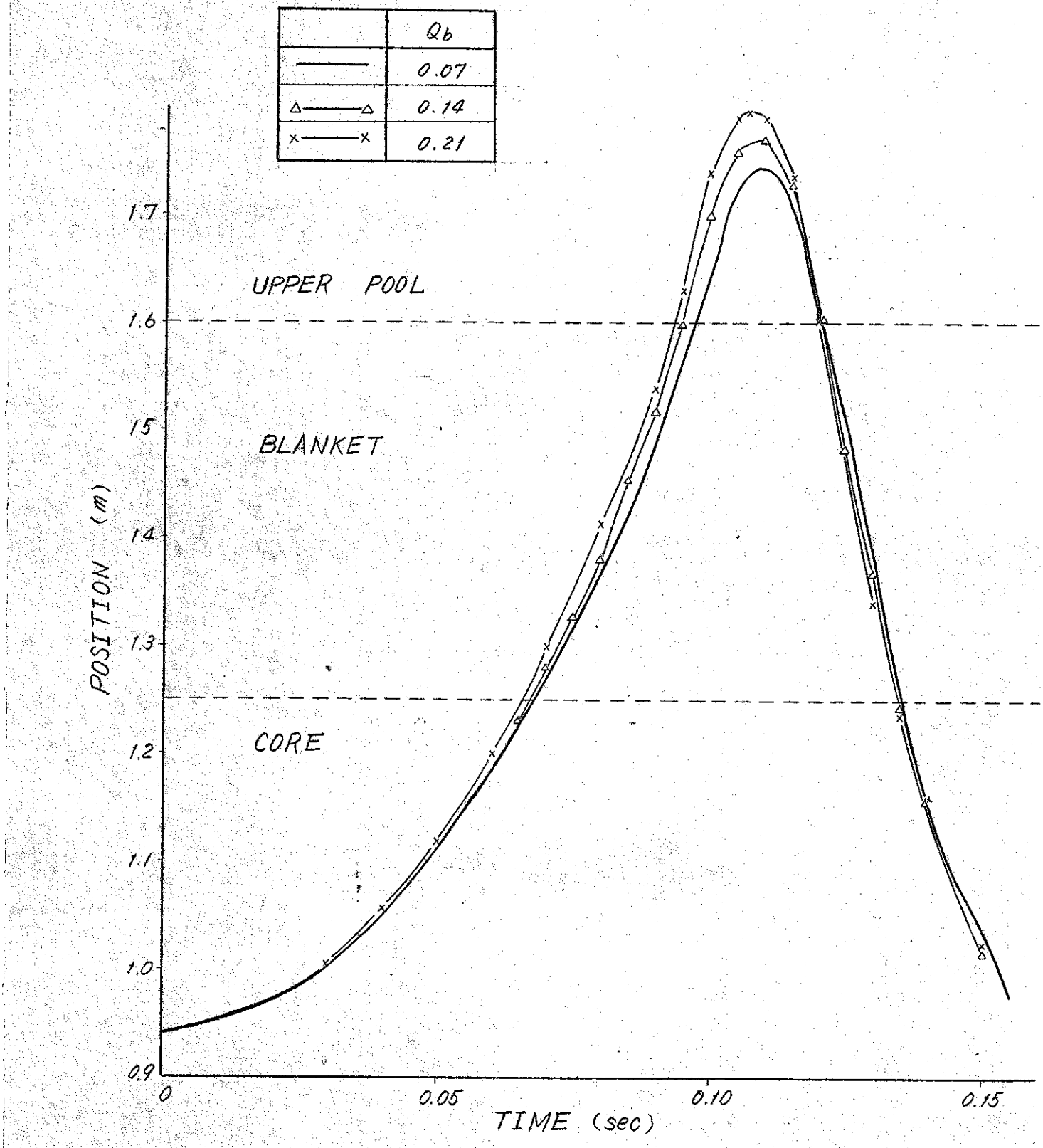

Fig. 6.12. Effect of blanket power rate on void position.

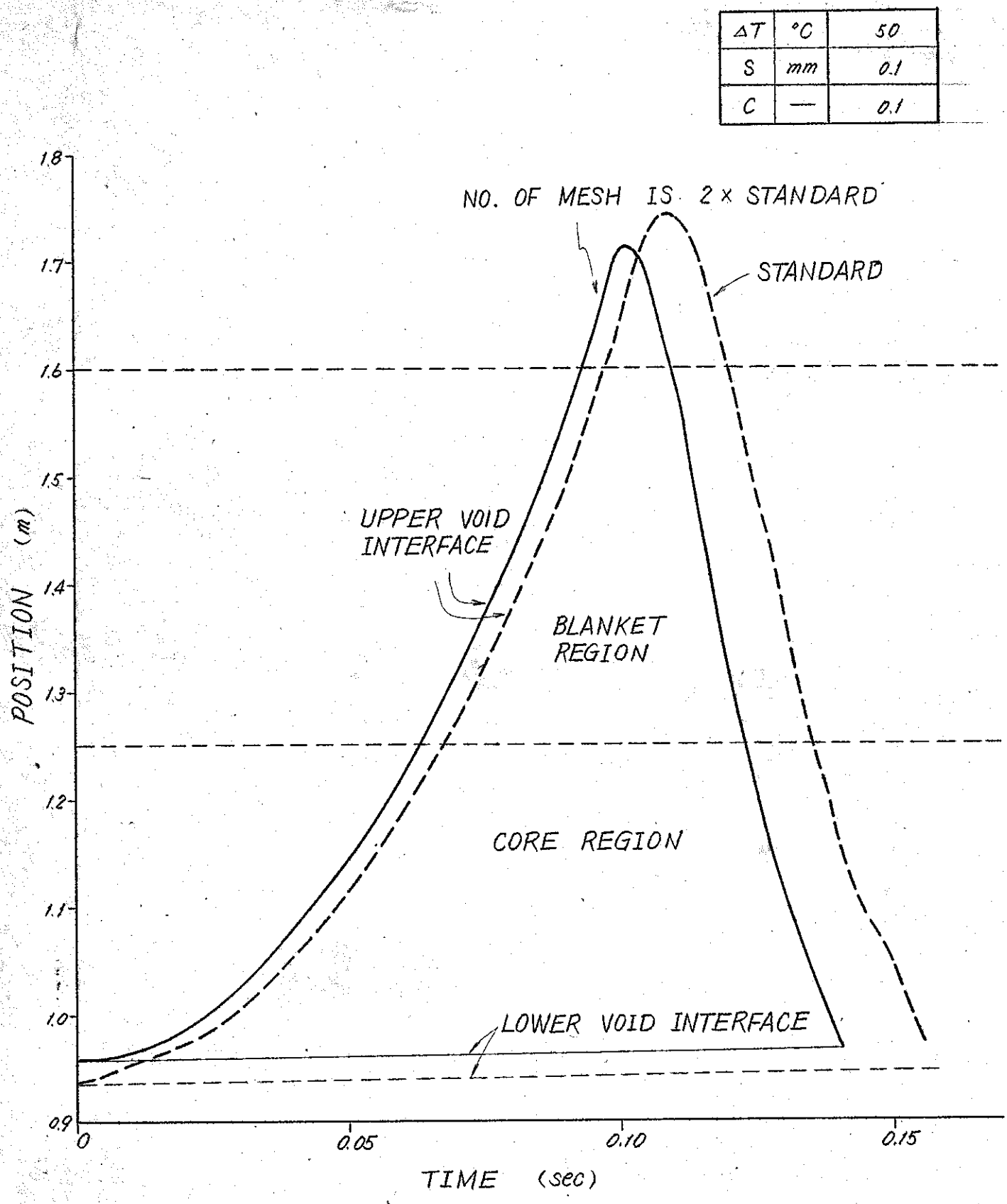

Fig 6.13. Mesh dependence of void interface position.

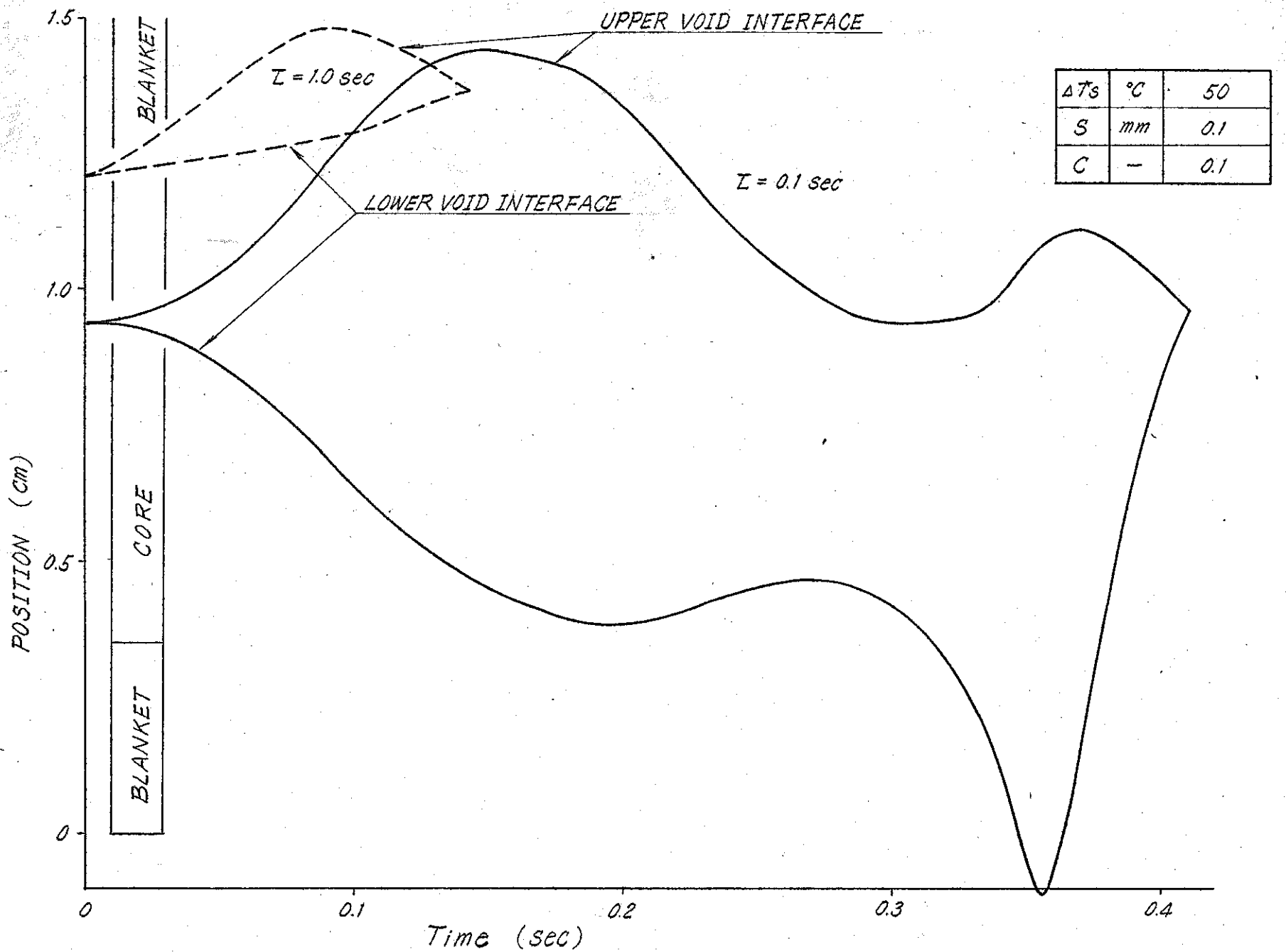

Fig. 6.14. Time dependence of void interface position in decrease of pressure at channel entrance.

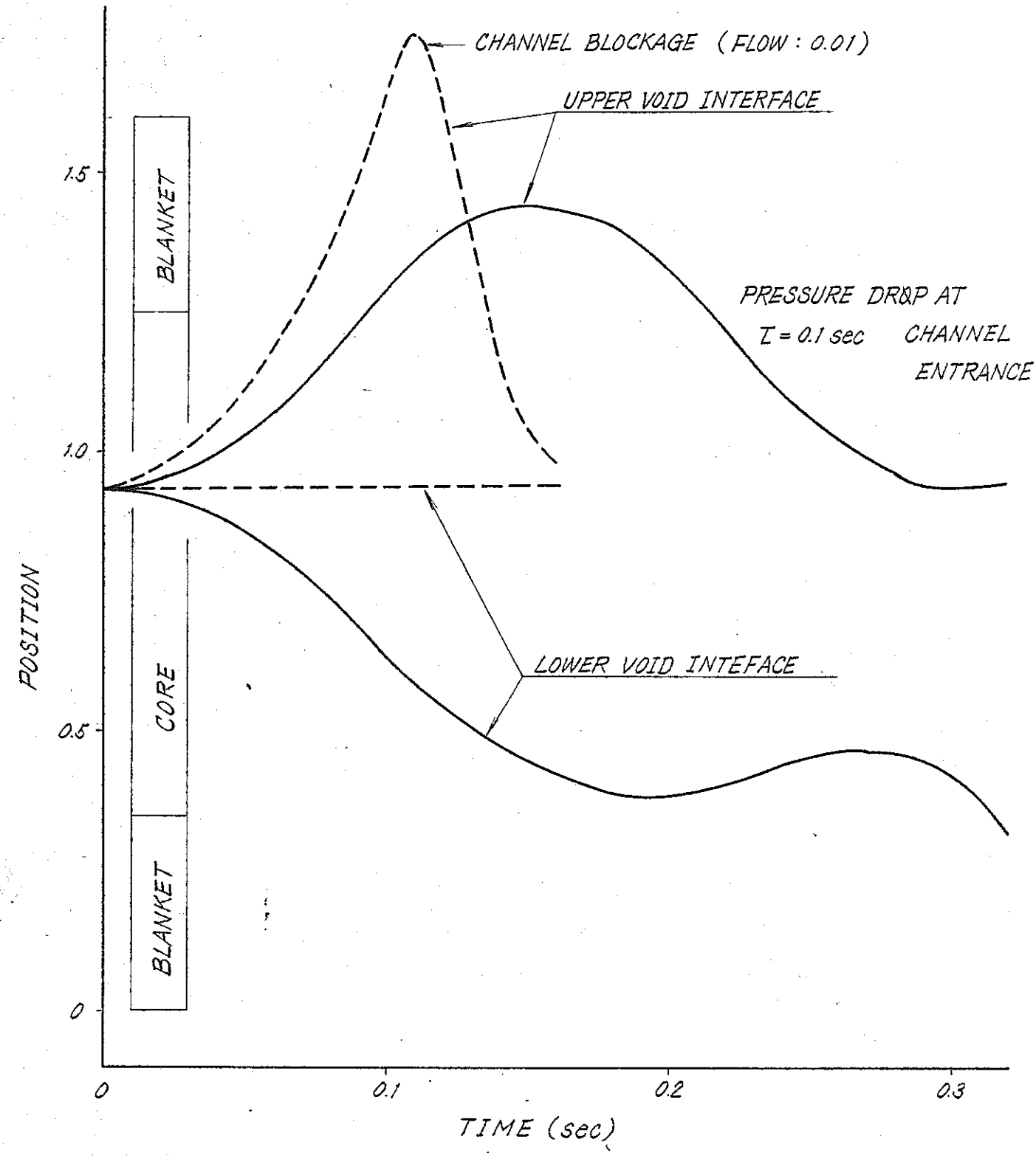

Fig. 6.15. Comparison between channel blockage and pressure drop accident.